An Investigation into Polybenzimidazoles as Anion Exchange Membranes

by

Kristen Jean Wing Yen Soo

B.Sc., McMaster University, 2009

Thesis Submitted in Partial Fulfillment
of the Requirements for the Degree of
Master of Science

in the
Department of Chemistry
Faculty of Science

SIMON FRASER UNIVERSITY

Summer 2013

Approval

Name: **Kristen Jean Wing Yen Soo**

Degree: **Master of Science**

Title of Thesis: ***An Investigation into Polybenzimidazoles as Anion Exchange Membranes***

Examining Committee:

Chair: David Vocadlo
Professor, Department of Chemistry

Steven Holdcroft
Senior Supervisor
Professor, Department of Chemistry

Tim Storr
Supervisor
Assistant Professor, Department of Chemistry

Vance Williams
Supervisor
Associate Professor, Department of Chemistry

Hogan Yu
Internal Examiner
Professor, Department of Chemistry

Date Defended: March 1, 2013

Partial Copyright Licence

Abstract

A study was done into three sets of polybenzimidazoles (PBIs). The first set is a quaternized PBI known as poly(1,3-dimethyl benzimidazolium) (P(DMBI)) that was shown to have anion exchange properties. The second set is a novel quarternized PBI that had additional methylation on the phenyl ring known as mesitylene-poly(1,3-dimethyl benzimidazolium) (Mes-P(DMBI)) which also had anion exchange properties. The last set is a series of blend membranes of PBI and Mes-P(DMBI)-OH^-, which showed that it was possible to synthesize a stable, hydroxide-conducting polymer.

The P(DMBI) membranes were synthesized with various counter-anions (I^-, Cl^-, Br^-, NO_3^-, HCO_3^- and OH^-) and they were mostly found to have low water uptake at high ion exchange capacities (IECs) and good conductivity values. They were also found to be thermally stable up to approximately 150°C. The hydroxide membrane was unstable due to membrane degradation, which provided the impetus to synthesize the second and third sets of PBIs mentioned above.

Mes-P(DMBI) is a novel polymer that was synthesized in order to attempt to create a stable hydroxide-conducting polymer. It was also synthesized with various counter-anions (I^-, Cl^-, Br^-, OH^-), and they were found to have much higher water uptake than their P(DMBI) counterparts. The hydroxide membrane was stable, but water-soluble, rendering it unusable as anion exchange membranes (AEMs).

The stability of the aforementioned Mes-P(DMBI)-OH^- prompted the synthesis of a series of blend membranes of PBI and Mes-P(DMBI)-OH^- with different IECs. This utilized the cross-linking and mechanical stability properties of PBI, combined with the hydroxide-conducting property of Mes-P(DMBI)-OH^- to make a stable, hydroxide-conducting membrane. The blend membranes were found to conduct hydroxide and to be stable in concentrated (2 M) $KOH_{(aq)}$ at 60°C over the period of a week, showing great promise for use in AEM fuel cells.

Dedication

This thesis is dedicated with love to all who have helped to make it possible: my dear parents, brother, and extended family; Grace Mosher; John Doan; The Point Community Church; the Simon Fraser University Choir; the many other friends who have supported me along the way; and to my Lord and Saviour Jesus Christ, who has sustained me along this journey.

“I can do all things through Christ who strengthens me.” – Philippians 4:13.

Acknowledgements

I would like to thank my supervisor, Professor Steven Holdcroft, for his guidance and support throughout this thesis. Special thanks also go to Professors Tim Storr and Vance Williams, my supervisory committee members.

I also extend my deepest thanks to the past and present members of the Holdcroft group, who have been very supportive during my time here. A special mention goes to Owen Thomas and Drs. Timothy Peckham and Mahesh Kulkarni for all of their thoughtful insight and hours spent helping me out.

This thesis would not have been possible without funding from Simon Fraser University and the Natural Sciences and Engineering Research Council.

My deepest and sincerest thanks to all of you.

Table of Contents

List of Tables

List of Figures

List of Acronyms

AEM	Anion Exchange Membrane
AEMFC	Anion Exchange Membrane Fuel Cell
AFC	Alkaline Fuel Cell
DMAc	Dimethylacetamide
DMF	Dimethylformamide
DMSO	Dimethylsulfoxide
DSSC	Dye-Sensitized Solar Cell
DVS	Dynamic Vapour Sorption
FTIR	Fourier Transform Infrared Spectroscopy
IEC	Ion Exchange Capacity
MeOH	Methanol
Mes-PBI	Mesitylene-poly(benzimidazole)
Mes-P(DMBI)	Mesitylene-poly(dimethylbenzimidazolium)
NMP	N-methylpyrrolidinone
NMR	Nuclear Magnetic Resonance
PBI	Poly(benzimidazole)
P(DMBI)-Br^-	Poly(dimethylbenzimidazolium) bromide
P(DMBI)-Cl^-	Poly(dimethylbenzimidazolium) chloride
P(DMBI)-I^-	Poly(dimethylbenzimidazolium) iodide
PEM	Proton Exchange Membrane
PEMFC	Proton Exchange Membrane Fuel Cells
TGA	Thermal Gravimetric Analysis

1. Introduction

1.1. Anion Exchange Membranes and their Applications

Anion exchange membranes (AEMs) are polymers that contain a fixed, immobile cation and a negatively charged anion. They have been shown to be stable in water and can be tuned to have different properties (i.e. stability, ion exchange capacity, flexibility, solubility, etc.) depending on their intended use. Often the positive charge is attained by using a quaternary nitrogen atom on pendant chains attached to the polymer backbone. The positively charged nitrogen is counterbalanced by a mobile anion, as shown in Figure 1.1 below as well as the examples described in this section.

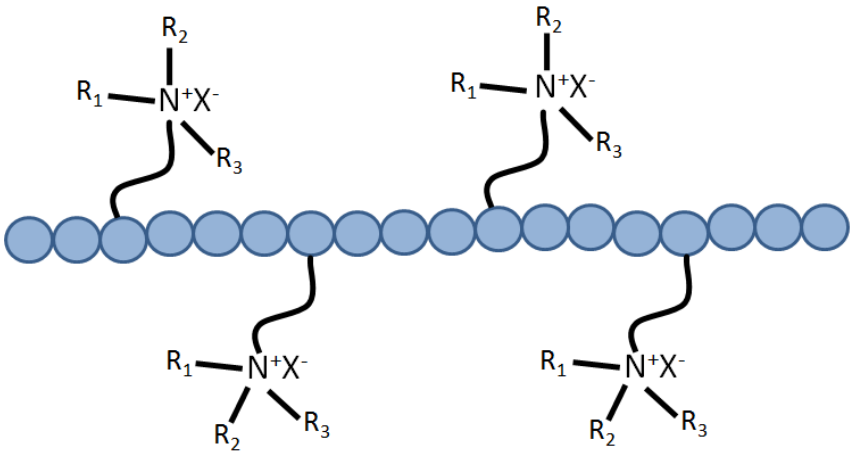

Figure 1.1: General structure of an AEM.

In general, when designing AEMs, consideration must be taken so that a membrane has a sufficiently high ion exchange capacity (IEC), which is the quantitative measurement of the number of charged sites in a polymer, as shown below in Equation 1. The multiplier of 1000 allows for the reporting of IEC in whole numbers.

$$IEC = \left(\frac{number\ of\ anionic\ sites\ per\ repeat\ unit}{molecular\ mass\ of\ one\ repeat\ unit}\right) x\ 1000 \quad (1)$$

The IEC must be high enough to allow for good ion transport, but also low enough that the membrane does not swell too much in aqueous solution. A very high IEC often results in membranes breaking upon immersion in water due to the high ionic content. A good IEC range for quaternary ammonium AEMs has been found to be ~0.9 – 1.4 meq g^{-1}. Also, membranes must usually take up a significant amount of water for complete dissociation, especially since model quaternary ammonium membranes have been shown to contain water that is not directly associated with the ionic groups. Their stability was also found to be lower when the membranes were not fully hydrated, which shows the importance of water to these membranes.[1]

AEMS have a broad range of applications such as ion exchange separators in vanadium batteries[2], electrodialysis[3] and filtration[4,5], dye-sensitized solar cells, and in alkaline anion exchange membrane fuel cells[1], as described below.

1.1.1. Filtration

AEMs are useful in filtration applications as they are stable in water, impermeable to positive ions, and can be tailored to be selective to specific ions. Recently, studies have looked at their potential use in nanofiltration applications, a field that is dominated by neutral and cation exchange membranes. Du and Zhao recently demonstrated that a cross-linked membrane of poly(N,N-dimethylaminoethyl methacrylate) and polysulfone (shown in Figure 1.2) could be used in filtration, and that changes in the relative amounts of each polymer, as well as reaction conditions, drastically affected membrane performance, showing again the tunability of AEMs.[4]

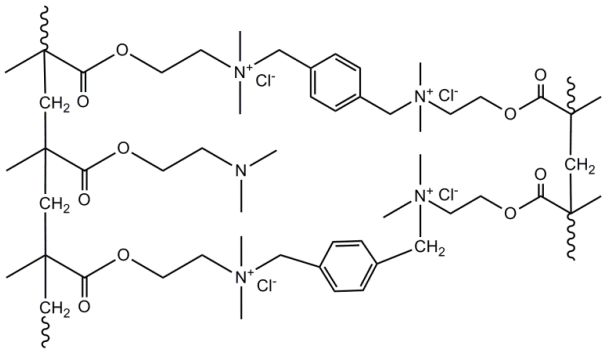

Figure 1.2: Cross-linked AEM synthesized by Du and Zhao.[4]

Another class of polymers that has been investigated for filtration is the polyimides, which have been used in engineering plastics since they are chemically and thermally stable. Due to their insolubility in most organic solvents, they were initially not suitable for use as AEMs, but they can be modified to include bulky groups, phenylene rings and flexible cross-links in order to become soluble. As an example, Kim and Tak describe the synthesis of a polyimide containing a pyridine group, whose structure is shown in Figure 1.3. This polymer was tested as a salt nanofiltration membrane and shown to have better salt retention properties than a comparable neutral polyimide membrane due to anion exchange with the cation.[6]

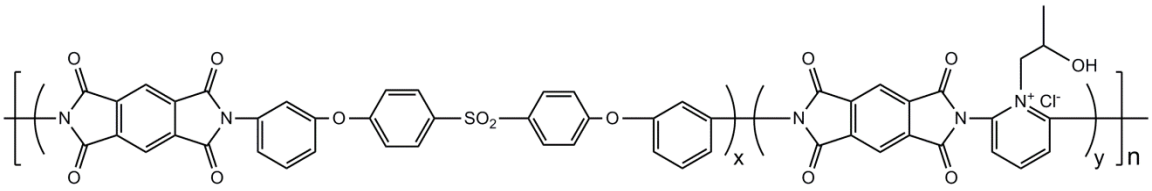

Figure 1.3: Basic structure of the soluble polyimide prepared by Kim and Tak.[6]

AEMs have also been employed to recover acid from wastewater solutions, as they allow for easy transport of anions across them, but not protons. Tongwen and Weihua used poly(2,6-dimethyl-1,4-phenylene oxide) (PPO) as a base polymer and through aryl and benzyl bromination, then cross-linking through amination, turned it into an AEM. They found that varying the amount of benzyl substitution affected the rate of acid recovery, while varying the amount of aryl substitution affected the membrane's

selectivity for the desired ions. This shows that AEMs are versatile and their properties are tunable.[7]

Singh et al. have recently devised a green synthesis for a hybrid organic-inorganic AEM using a sol-gel reaction in water and poly(vinylalcohol) (PVA), whose structure is shown below in Figure 1.4. This type of membrane is quite interesting because the inorganic segment imparts mechanical and thermal stability to the membrane, while the organic segment allows for flexibility and the desired reactivity of the polymer. It is fairly hydrophobic and mechanically strong, meaning it represents a new class of AEMs.[8]

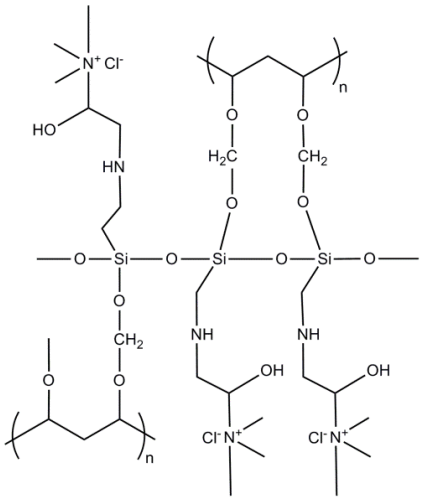

Figure 1.4: Structure of the inorganic-organic hybrid AEM synthesized by Singh et al.[8]

1.1.2. Electrodialysis and Separation

Electrodialysis is a process by which ions are moved from one solution to another via an applied electric potential. This allows for the concentration of ions in order to recover them later. The most widely used application for this technique is in desalination of saltwater to make it potable, and purification of the resulting brine for salt. However, in recent years, this technique has also been used to recover acids and bases from industrial wastewater, the production of acids and bases from their salts, and even energy generation.[9]

A conventional electrodialysis set-up is shown below in Figure 1.5, where both cation exchange membranes (CEMs) and anion exchange membranes (AEMs) are alternated between the anode and cathode. When an electric potential difference is applied, the feed solution flows through the chamber between the anion and cation membrane, with the result that the chambers will eventually become concentrated with ions.

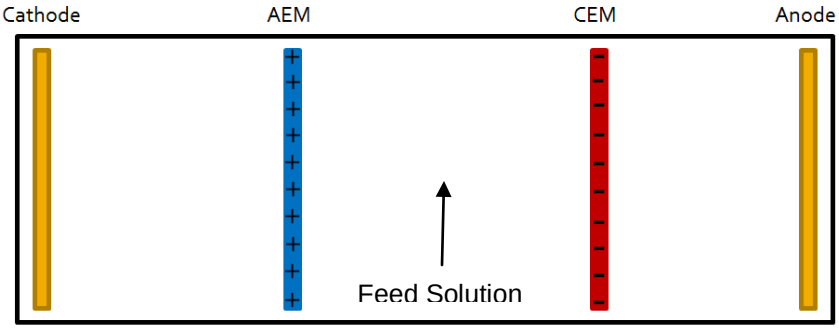

Figure 1.5: A conventional electrodialysis set-up.

1.1.3. Batteries

In vanadium batteries, AEMs can be used to separate the cathode and anode solutions in order to prevent them from reacting with one another.[10] It is crucial in these batteries that the membrane is impermeable to vanadium ions to prevent crossover, which causes the battery to self-discharge. This has been shown to be a problem with the Nafion membranes that were used previously. It was theorized that an AEM could be used since they contain fixed cations which would repel the vanadium cations and thus prevent them from crossing over. Qiu et al. prepared such an AEM by grafting an aminated monomer onto an ethylene tetrafluoroethylene (ETFE) membrane, and found that it had a significantly lower vanadium crossover and a generally better performance than Nafion, making it viable for use in these types of batteries. The structure of their AEM is shown below in Figure 1.6.[2]

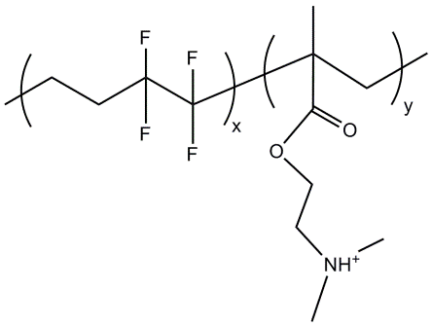

Figure 1.6: Structure of the grafted ETFE polymer prepared by Qiu et al.[2]

1.1.4. Dye-Sensitized Solar Cells

Another area in which these membranes are starting to find applications is as solid electrolytes in dye-sensitized solar cells (DSSCs). These types of solar cells were first developed by Grätzel in 1991, and consist of a film of TiO_2 particles coated with a monolayer of a charge-transfer dye. A current is generated when light hits the dye molecule, which absorbs a photon and then ejects an electron into the semiconducting layer. The circuit is completed by means of the presence of a reducing agent that regenerates the dye.[11]

Classic organic photovoltaic devices used one material for both light harvesting and charge carrier transport, and it was a challenge to find materials that satisfied both of these properties. The development of the DSSC allowed for the use of separate materials for light harvesting and carrier transport, which opened up a promising avenue for optimization of solar cells for commercial energy use.[12] The ionic conductivity of solid electrolytes ranges on the order of 10^{-8} to 10^{-5} S cm^{-1} for solid electrolytes at room temperature, depending on the nature of the electrolyte. This conductivity can be increased up to the order of 10^{-4} – 10^{-3} S cm^{-1} with the addition of solvents and/or ionic liquids.[13-15] The conductivities of liquid electrolytes typically range from 10^{-4} to 10^{-3} S cm^{-1}, but despite higher conductivity, research in this field is turning more and more to solid electrolytes as liquid electrolytes have several problems such as leaking, volatility and viscosity. Solid polymer electrolytes therefore represent an attractive alternative as they do not suffer from the issues mentioned above.

1.2. Anion Exchange Membrane Fuel Cells (AEMFCs)

A fuel cell is an apparatus that can directly convert chemical energy into electrical energy, and differs from a traditional galvanic cell in that it does not require recharging to provide a continuous current as long as a steady supply of fuel is available[16]. This property has made them attractive as alternatives to internal combustion engines in automobiles[17-19] and for stationary power generation as well.[19]

Fuel cells that use hydrogen have been studied extensively in recent years because their only by-products are water and heat, and as such, they are viewed as a source of clean energy.[5] Even though they are too expensive for widespread commercial use, the declining supply of fossil fuels and the environmental issues associated with greenhouse gas emissions have driven researchers to focus on improving them to address these issues. The main costs that hold back fuel cells from wider use come from the expensive catalysts, the fuel, and the polymers used as solid electrolytes. Most efforts in recent years have focussed on moving toward cheaper catalysts and membranes, as well as attempts to improve the overall efficiency of the fuel cell.

All fuel cells consist of an anode, a cathode, and an electrolyte. In the case of hydrogen fuel cells, hydrogen gas is oxidized at the anode and the oxidant gas (either oxygen or air) is reduced at the cathode. The electrolyte serves as a conduit for ions to flow from one side to the other, and a current is produced from an external electric circuit. This is shown below in Figure 1.7 for an anion exchange membrane fuel cell, in which hydroxide ions are the conductive species and a mixture of oxygen and water gasses are the fuel.

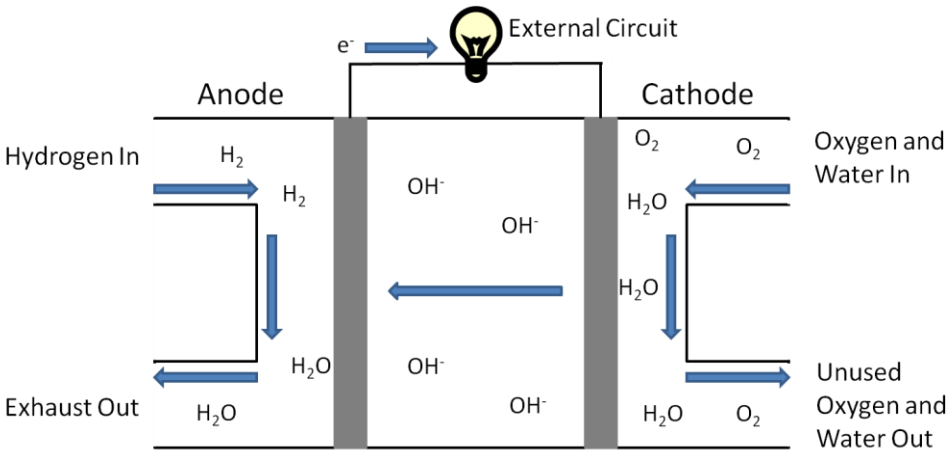

Figure 1.7: General schematic of an anion exchange membrane fuel cell.

The vast majority of literature on polymer membranes for hydrogen fuel cells has focussed on negatively charged proton exchange membranes (PEMs), but the body of literature on anion exchange membranes is growing. In recent years, many groups have looked at using polymers as AEMs in alkaline fuel cells. The precursor to the AEMFC is the alkaline fuel cell (AFC), in which the cathode and anode are separated by a liquid electrolyte instead of a solid one. The electrolyte is usually aqueous potassium hydroxide. The advantages to using this type of fuel cell are that the oxygen reduction reaction in basic media is much faster, and so cheaper cathode catalysts such as nickel and silver can be used, as opposed to the expensive noble metal catalysts that must be used for proton exchange membrane fuel cells. Various issues with AFCs include electrolyte leaking and electrode poisoning by the formation of carbonic acid from the reaction of KOH with carbon dioxide in the air, which requires the fuel materials to be of high purity.[20] AEMs are a viable alternative as a solid electrolyte due to the fact that they do not suffer from the leaking issue, and there is no possibility of carbonate precipitation since the cations are attached to the polymer and thus immobile. A brief discussion of some recent advances in literature in this area is described below.

Robertson et al. recently demonstrated that it was possible to tailor the synthesis of a polymer for various intended purposes, but most importantly for AEMFCs. They were able to synthesize the polymer in the hydroxide form with no post-polymerization

modifications through addition of tetraalkylammonium groups to the monomer prior to polymerizations. The structure is shown below in Figure 1.6. [21]

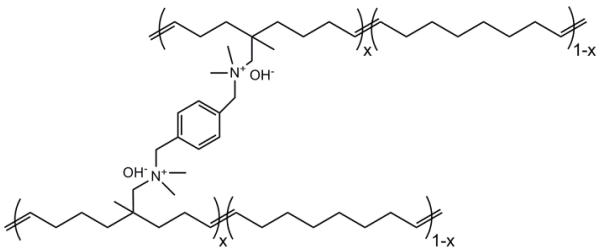

Figure 1.8: Structure of the AEM synthesized by Robertson et al.[21]

Another avenue that has been pursued is the amination of the polymer Nafion, which is the standard polymer used in proton exchange membrane fuel cells owing to its high thermal, mechanical and chemical stability. It is a perfluorinated block polymer with a triflic acid-like pendant group and an ionic morphology that leads to high water-saturated conductivities. Specifically, the morphology is such that the hydrophobic and hydrophilic blocks are phase-separated on the nanoscale when the membrane is dry, and when hydrated, the hydrophilic regions form channels that allow for proton dissociation and therefore conductivity.[22] Surprisingly, this avenue of Nafion modification has not been widely explored until very recently. Salerno et al. synthesized a chemically modified Nafion in which dimethylpiperazinium cations were added to it in order to make it an AEM (structure shown below in Figure 1.4). The membrane was found to be nearly identical to Nafion in terms of morphology, and was also thermally, chemically and mechanically stable at operating conditions. The hydroxide conductivity was found to increase with temperature and ranged between 1.33 – 11.5 mS cm^{-1}. Moreover, the conductivity was recoverable upon dehydration and reheating of the membrane.[23]

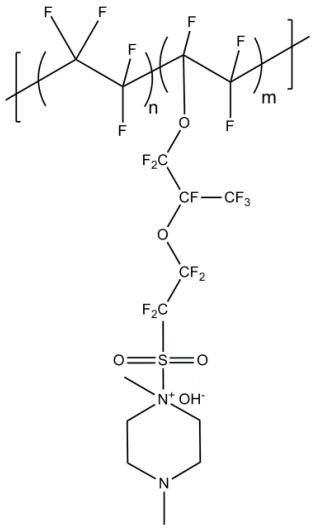

Figure 1.9: Chemically modified Nafion AEM made by Salerno et al.[23]

Another solution that has been examined is the doping of polybenzimidazole, or PBI (see Figure 1.8 for structure), with $KOH_{(aq)}$ to turn it into an AEM. It has been doped with phosphoric acid and successfully used as a PEM,[24] and is also very durable in alkaline media, so various groups have investigated its viability as an AEM. Hou et al. tested the durability of a PBI/KOH membrane in an alkaline direct ethanol fuel cell (ADEFC) and its conductivity was found to decrease by 43% after 100 hours of operation and was stable for 336 hours at 60°C.[25] In another paper, they found that KOH molecules were embedded evenly in the PBI matrix, which likely contributes to the high conductivity in these membranes.[26] Recently, Matsumoto et al. tried wrapping hydroxide-doped PBI around carbon nanotubes to use it as an electrocatalyst in AEMFCs to help improve their power densities. When it was tested in a membrane electrode assembly, it was found that the PBI layer worked well as a hydroxide-conducting path.[27]

Despite all of these advances, to the best of our knowledge, a stand-alone (i.e. undoped), hydroxide-conducting AEM has not been synthesized. The polymers that have been synthesized for this purpose suffer from degradation after prolonged periods of time, and thus are not suitable for commercial use.[28-29] The main drive behind this thesis project was toward synthesis of such a membrane, as this represents the next stage of development toward the commercialization of AEMFCs.

1.3. Ionic Liquids

Ionic liquids are salts that are liquid at room temperature.[30] They were first reported by Chum et. al in 1975 as a solvent in which electrochemical reactions could be studied.[31] They have since been used extensively as aprotic solvents for various chemical reactions; moreover, since they are often conductive, they have been studied for use as electrolytes in electrochemical applications.

The thermal and chemical stability of ionic liquids has led to their use in a number of electrochemical applications.[32-33] Composites of ionic liquids imbibed in polymeric matrices have been investigated,[32] as have polymers with tethered ionic liquid moieties, derived from vinyl-based monomers, although the polyvinylic nature of the backbone is unlikely to resist high water uptake at high IEC levels. The conductivity of poly(benzimidazole) : acid adducts in the dry state has been reported,[34-35] but in these systems the acid elutes from the polymer in the presence of water.

One class of ionic liquids that has recently been explored are nitrogen-containing heterocycles, such as imidazoles. They can be synthesized through the reaction of alkyl halides with imidazole to yields ionic liquid imidazolium salts. The halides can be easily exchanged with other anions (e.g., PF_6^-, BF_4^-, NO_3^-) depending upon the desired properties.

The polymers studied in this thesis can be thought of as polymeric forms of ionic liquids, in that they contain the imidazole group and have electrochemical properties, and as such their properties are sometimes compared to those of ionic liquids of similar structure.

1.4. Poly(benzimidazole) (PBI)

PBI is a well-known polymer in the thermochemical industry. It is thermally stable up to approximately 650°C, oxidatively stable, and is also non-flammable, which has led to its use in thermal protective clothing and as an asbestos replacement.[36] Its structure is shown below in Figure 1.8.

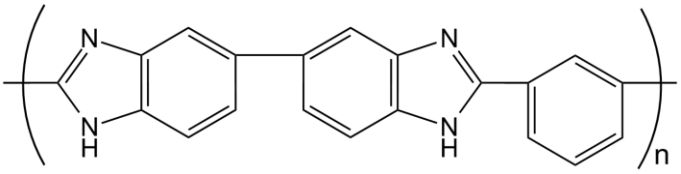

Figure 1.10: Structure of PBI.

In recent years, studies have investigated doping PBI with various acids in order to investigate its ionic conductivity. One of the first studies was done by Aharoni and Signorelli, who found that PBI salts of monoprotic acids performed very poorly as ionic conductors.[34] However, later studies by Wainwright et al. with amphoteric ions were much more promising, and showed good conductivity that increased with increasing acid concentration.[37] The acids were found to dissolve in the membrane, and a doping level of 50% was possible without damaging the polymer. The conductivity was also found to increase with increasing water content. Initial fuel cell tests using a methanol-powered fuel cell showed that the PBI membrane was stable for at least 200 hours at 150°C (quite high for a fuel cell) in the presence of hydrogen, oxygen and platinum, which were very promising results. In addition to this, it was found to have lower permeability to methanol than other electrolytes.[38]

H_3PO_4-doped PBI systems have been examined extensively for high temperature proton exchange membrane fuel cells (PEMFCs),[38-39] but anionic conductivity is secondary to the high proton conductivity of the phosphoric acid.

PBI is the base polymer for all compounds studied in this work.

1.5. Poly(dimethylbenzamidazolium) X^-

Alkylation of PBI has been reported in literature, but the intention was to evaluate the effects of N-substitution upon thermal, mechanical and gas permeability,[40-45] rather than ion conductivity.

In 1993, Hu et al. synthesized poly(dimethylbenzimidazolium) iodide (P(DMBI)-I^-), an alkylated polybenzimidazole whose structure is shown below in Figure 1.9. The intent

was to observe the effect of alkylation on the polymer's solubility in organic solvents, as well as its thermal and mechanical properties, since PBI is insoluble in many organic solvents. It was found that alkylation increased its solubility in dimethylsulfoxide (DMSO) and N-methylpyrrolidinone (NMP), likely owing to the fact that alkylation removed the interchain hydrogen bonding that is present in PBI. The polymer was also found to have much lower thermal stability than PBI; however, no measurements of its ionic conductivity were performed.[40] The impetus behind this work was the belief that this polymer could be used as an AEM due to its charged backbone and iodide ion, and that if it could be synthesized and found to be conductive, it would represent an entirely new class of AEMs in which the backbone, and not a pendant group, carried the mobile anion.

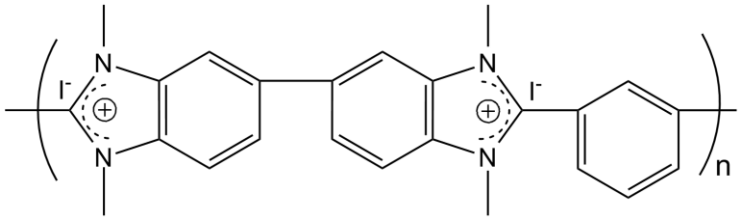

Figure 1.11: Structure of P(DMBI)-I-.

The subject of this thesis is the successful synthesis and characterization of P(DMBI)-I^-, its conversion to other anionic forms, and its further chemical modification to produce a chemically stable hydroxide-conducting polymer.

2. P(DMBI)-X^- Anion Exchange Membranes

This section is partially reprinted from:

Owen D. Thomas, Kristen J. W. Y. Soo, Timothy J. Peckham, Mahesh P. Kulkarni, Steven Holdcroft, Anion conducting poly(dialkyl benzimidazolium) salts. *Polymer Chemistry*, **2011**, 2, 1641-1643.

2.1. Contributions

I worked with Owen Thomas and Mahesh Kulkarni to synthesize PBI and P(DMBI)-I^-. I cast all of the membranes and carried out all anion exchange conversions, conductivity analyses, IEC measurements and other characterization experiments. I also edited all drafts of the manuscript. Dev Sharma performed the TGA measurements. Owen Thomas calculated λ, [X^-] and μ'_{X^-}.

The data that were reported in the paper include all of Section 2.4.1, and Table 2 with all associated observations in Section 2.4.3.

2.2. Overview

This section of the thesis presents the work that was done to synthesize and characterize the charged polymer poly(dimethylbenzimidazolium) in different anionic forms, known as P(DMBI)-X^-.

2.3. Materials Used

2.3.1. Polybenzimidazole (PBI)

All of the polymers used in this work were based on PBI, which can be synthesized in high molecular weight through the condensation of a tetraamine and a dicarboxylic acid, as shown below in Figure 2.1.

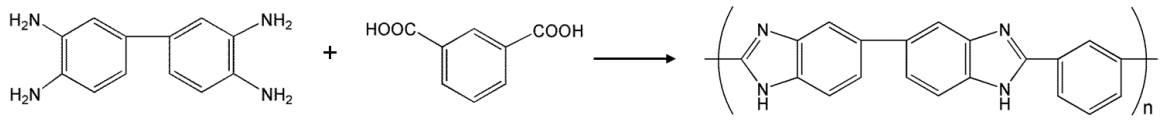

Figure 2.1: Scheme for the synthesis of PBI used in this work.

2.3.2. P(DMBI)-X^-

P(DMBI)-X^- is the primary polymer upon which experiments were conducted. The polymer is initially synthesized in the iodide form through a two-step reaction in which PBI is deprotonated, then methylated using methyl iodide, as shown below in Figure 2.2.

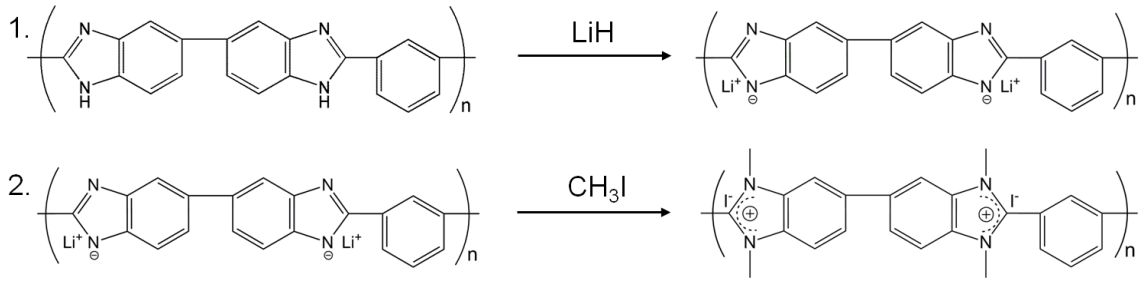

Figure 2.2: Scheme for the synthesis of P(DMBI)-I^-.

2.4. Results and Discussion

2.4.1. Polymer Synthesis and Basic Analysis

PBI was synthesized using the procedure outlined by Iwakura et al.[46]

P(DMBI)-I^- was synthesized using the procedure outlined by Hu et al.[40]

^{1}H NMR spectra for both compounds were found to be consistent with literature results. The PBI spectrum is shown in Figure 2.3 and the P(DMBI)-I^{-} spectrum is in Figure 2.4. The two singlets in the P(DMBI)-I^{-} spectrum (4.20, 4.13 ppm) integrate to 5.5 and 6 protons (where 6 would be expected for each one), and correspond to the two methyl groups on P(DMBI)-I^{-}. Of note is that they are not found in the PBI spectrum, which is evidence of methylation. Also, the PBI singlet at 13.3 ppm (which corresponds to the PBI imidazole protons) is not present in P(DMBI)-I^{-}, indicating that these protons have been replaced.

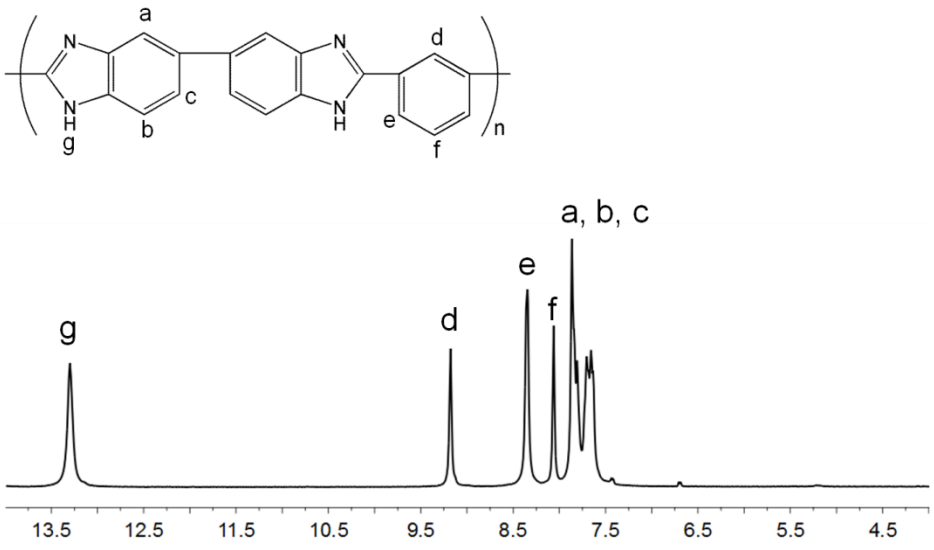

Figure 2.3: ^{1}H NMR spectrum of PBI.

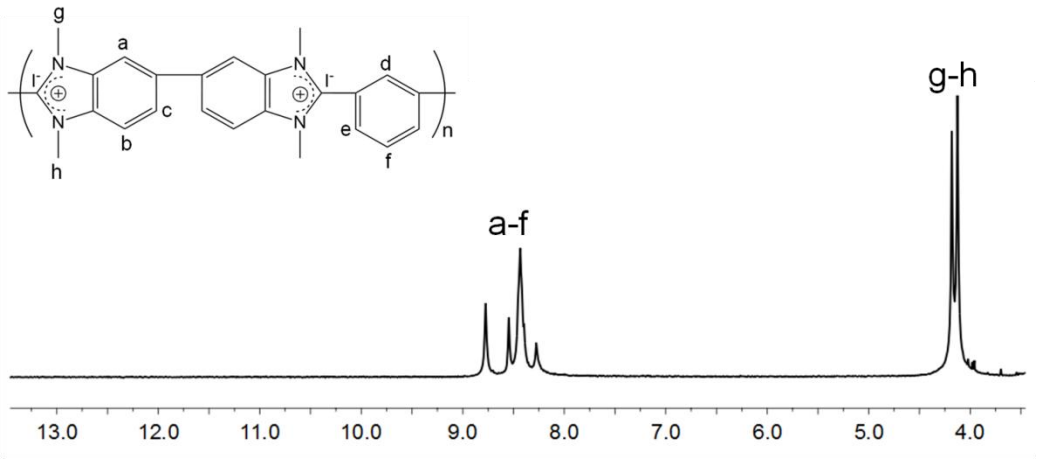

Figure 2.4: ^{1}H NMR spectrum of P(DMBI)-I^{-}.

The degree of methyl substitution on P(DMBI)-I^{-} was also calculated by comparing the ratio of the integrals of peaks g and h to those of peaks a – f as a whole, and it was found that 88-93% of the available nitrogen atoms of PBI were methylated. The technique of using NMR integration to quantify the number of protons is accurate to within 0.5% as demonstrated by Bauer et al.[47]

IR spectra of PBI and P(DMBI)-I^{-} are shown in Figure 2.5. Both polymers contain C=N/C=C groups (~1620 cm^{-1}) and exhibit an in-plane deformation of the benzimidazole ring (~1440 cm^{-1}). PBI contains a unique peak at ~3200 cm^{-1} correlating to an N-H stretch that is not present in P(DMBI)-I^{-}. The P(DMBI)-I^{-} spectrum also displays a new peak at 1216 cm^{-1} that corresponds to a C-N stretch from the new methyl groups. There is also a water peak at 3450 cm^{-1}. The new peaks provide additional evidence for the methylation of the nitrogen atoms in the benzimidazole system.

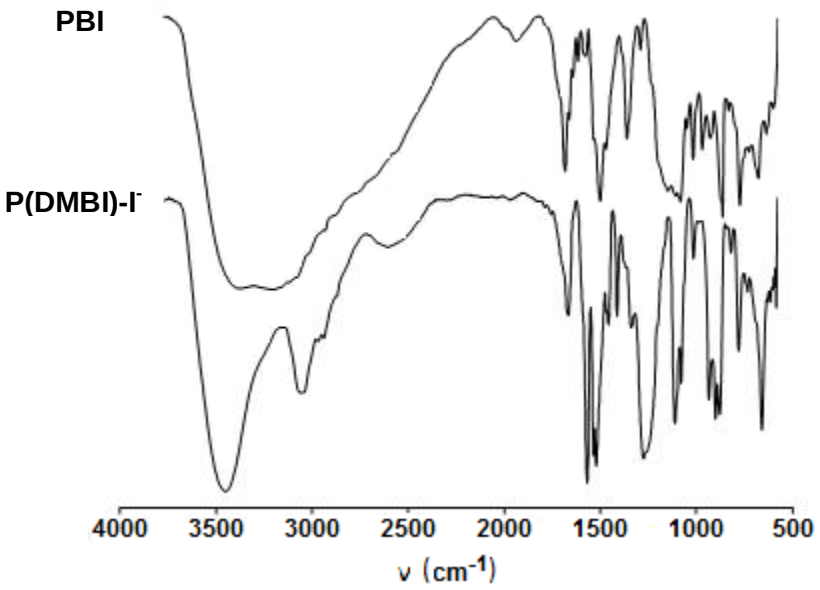

Figure 2.5: IR spectra of PBI and P(DMBI)-I⁻.

2.4.2. PBI Properties

A thermal gravimetric analysis (TGA) plot for PBI is shown in Figure 4, and it was found to be stable up to ~650°C, and then lost ~10% of its mass up to 850°C. This is consistent with literature results attesting to its high thermal stability.[48-50]

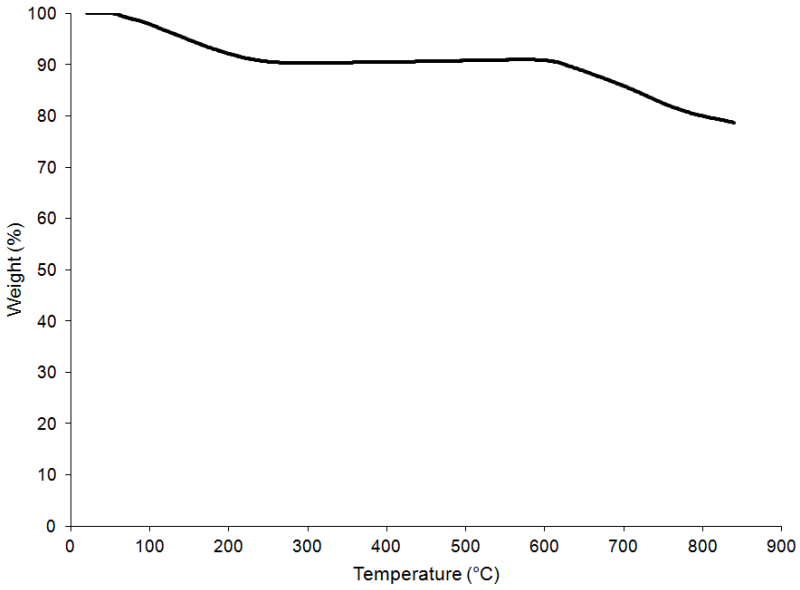

Figure 2.6: TGA plot for PBI under nitrogen at a heating rate of 10°C/minute.

PBI was found to have a water mass uptake of 32 ± 3%.

2.4.3. P(DMBI)-X^- Properties

Solvent absorption tests were done on P(DMBI)-I^- membranes in order to determine the effect of solvent on conductivity. The results are shown in Table 1. The P(DMBI)-I^- membrane was found to absorb solvents in the order of acetonitrile < water < propylene carbonate. Of note is that the membrane does not absorb a lot of water by mass (10%), but this amount of water caused its volume to increase by almost 30%. The opposite relationship is observed for both acetonitrile and propylene carbonate, as the polymer did not swell a lot despite absorbing approximately twice as much solvent by mass. This indicates that the behaviour of the polymer is solvent-dependent. Lastly, both acetonitrile and propylene carbonate do not appear to be effective plasticizers because when the membrane has fully absorbed either of those solvents, its conductivity is a full order of magnitude lower than when it has absorbed water. Since conductivity is dependent on the ability of the solvent to solvate and dissociate the anions from the positively charged polymer backbone, it is unsurprising that acetonitrile and propylene carbonate, not being ionic solvents like water, would not be able to accomplish this effectively.

Table 1: Solvent absorption of P(DMBI)-X^-.

Solvent	Mass Uptake (%)	Volume Uptake (%)	Conductivity (mS cm^{-1})
Water	10 ± 2	28 ± 3	3.3 ± 0.4
Acetonitrile	6 ± 2	3 ± 1	0.25 ± 0.08
Propylene carbonate	32 ± 4	18 ± 2	0.30 ± 0.05

P(DMBI)-I^- membranes were converted to other anionic forms as described in Section 2.6.3.2. All tested anionic forms of P(DMBI)-X^- were found to be mechanically stable except for the hydroxide form, which broke apart almost instantly upon immersion of P(DMBI)-I^- in hydroxide solution. This was the motivation for the work presented in Chapter 3, and is discussed more fully in that chapter.

Thermal gravimetric analysis was performed on P(DMBI)-I^-, P(DMBI)-Br^- and P(DMBI)-Cl^- (experimental conditions listed in Section 2.6.2.3) and their TGA curves are shown below in Figure 2.7. P(DMBI)-I^- is stable up to 160°, and has a mass loss of 10% up to ~95% which is likely water (which showed up in the IR spectrum). This water is most likely absorbed from ambient air. It then loses ~45% of its mass between 160 – 400°C, and then decomposes above 550°C. It is likely that the ~45% mass loss is due to the loss of two methyl iodide groups, as they correspond to 46% of the molar mass of the polymer backbone. Henkensmeier et al. have done TGA studies coupled with a GC/MS on this polymer and confirmed that this is the product lost at this temperature range.[51]

P(DMBI)-Br^- is stable up to 216°C, and shows a mass loss of ~13% up to 93°C, and then it was stable up until 216 – 397°C where it lost ~33% of its mass. The polymer then lost another 8% of mass between 397 – 487°C, followed by a sharp decrease in mass between 487 – 550°C and then decomposes past that temperature. Again, it is likely that the first mass loss is residual water, and the second mass loss of ~33% is

likely due to methyl bromide loss (which in theory makes up 36% of the mass of the polymer).

The P(DMBI)-Cl^- curve shows three small mass losses (totalling ~13%) up to 86°C, and is then stable up to 212°C where it loses ~18% of its mass up to 328°C and then loses another ~12% of its mass between 328 – 394°C. The polymer then slowly decomposes at higher temperatures. The negative values of weight loss and the fact that there are multiple mass losses before 86°C (which would be water) for this curve are likely due to the balance shifting during the experimental process. The first mass loss of ~13% is again likely water, and the mass loss of ~18% is likely the loss of methyl chloride from the polymer backbone (which comprises 22% by mass of the polymer). Again, Henkensmeier et al. confirmed this in their TGA experiments on this polymer.[51]

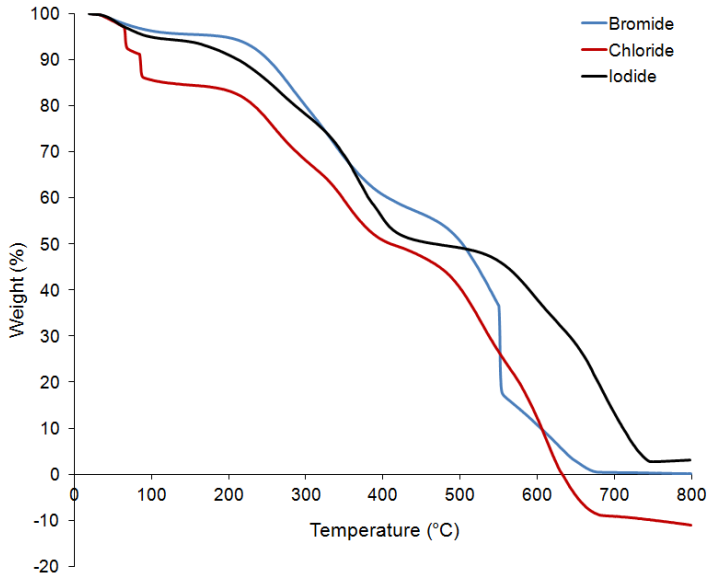

Figure 2.7: TGA plots of P(DMBI)-I^- (black curve), P(DMBI)-Br^- (blue curve) and P(DMBI)-Cl^- (red curve).

The TGA curves for P(DMBI)-Br^- and P(DMBI)-Cl^- both found to have more than two observable mass losses; however, it is notable that both polymers are stable past 200°C, which is not the case for the iodide membrane (which begins to decompose past 160°C). Also, it is likely that at higher temperatures, the polymer chain cleaves to form ammonia, hydrogen cyanide and nitrogen, as well as more condensed heterocyclic

species[52-53]; however, determining the exact nature of these products was not deemed important for this thesis, as the purpose of the TGA experiments was to determine the thermal stability of these compounds.

Overall, the TGA results for the P(DMBI)-X^- membranes show a much lower decomposition temperature than PBI, given their chemical nature. This supports the postulate that methylation of the nitrogen atoms prevents interchain bonding between the P(DMBI)-I^- chains that is present in PBI, because decreased interchain bonding would contribute to a lower thermal stability. Both the P(DMBI)-Br^- and the P(DMBI)-Cl- polymers are stable past 200°C, while the iodide membrane decomposes past 160°C. By comparison, many ionic liquids containing the imidazolium group are stable to at least 200°C or higher[54-59] although a few do decompose as low as 145°C.[60] Also, the losses of methyl halide have been verified by Henkensmeier et al., who did recent TGA experiments on P(DMBI)-X- and P(DMBI)-Cl- in which the TGA was coupled with a GC/MS for product analysis.[51]

The reproducibility of TGA results depends on six things: calibration, furnace cleanliness, sample preparation, temperature range, temperature scanning rate and the sample atmosphere.[61] For the experiments run for this thesis, the TGA machine had been recently calibrated, the samples were all prepared in the same way (pieces of cast films) and all had weights within 5 mg. of each other, the temperature range and scanning rate were the same for all experiments, and the sample atmosphere was consistent, and thus it is very likely that these experiments are reproducible. The furnace cleanliness at the time of the experiments is not known, but provided the instrument is cleaned regularly, this would likely not be a large contributor to reproducibility.

Membrane properties of P(DMBI)-X^- as a function of X^- are shown below in Table 2. Each one has a different IEC because this is a measure of the number of ionic sites per mass of the repeat unit, as shown in Equation 1 in Section 1.1.

It was found that the Br^-, HCO_3^-, I^- and NO_3^- membranes had relatively low water content, as evidenced by their low λ values of 2, 3, 2 and 5, respectively (where λ = moles of H_2O per mole of N^+). However, P(DMBI)-Cl^- was found to reproducibly have a very high λ of 167, which is quite surprising since it is two order of magnitudes higher

than the corresponding values for the Br^- and I^- membranes. This large difference in values can be explained by the fact that in alkali halide salts, the free energy of hydration (ΔG_{hyd}) increases as the difference in size between the anion and cation increases (where the size difference increases from $I^- < Br^- < Cl^-$). This trend is the same for the anion hardness, which increases the ionic character of the imidazolium-halide pair and thus the polymer's hydrophilicity, which leads to the observed high λ value for P(DMBI)-Cl^-.[62]

Table 2: Membrane properties of P(DMBI)-X^- as a function of X^-.

X^-	IEC (meq/g)	λ	σ_X (mS cm^{-1})	$[X^-]$ (M)	μ'_{X^-} (10^5 cm^2 V^{-1} s^{-1})	$\mu_{X^-}^{\infty g}$ (10^5 cm^2 V^{-1} s^{-1})
Cl^-	4.16	167	7.6 ± 1.1	0.32	24.62	79.1
Br^-	3.48	2	3.2 ± 0.4	4.32	0.77	80.9
I^-	2.97	2	3.3 ± 0.4	4.31	0.79	79.6
NO_3^-	3.72	3	4.9 ± 0.4	4.96	1.02	74.0
HCO_3^-	3.74	5	8.5 ± 0.5	3.68	2.40	-
I_3^-	1.50	<1	2.7 ± 0.3	3.29	0.85	-

The conductivities of these membranes in the fully hydrated wet state are at least 2 orders of magnitude greater than in the dry state, as seen in Table 2. The data also showed unexpected differences as a function of anion. For example, σ is similar for the I^- and Br^- membranes, even though the latter has a higher IEC. Also, the water uptake and IEC values are similar for the NO_3^- and HCO_3^- membranes, but the latter has a significantly higher conductivity. It was also observed that the HCO_3^- and Cl^- membranes had nearly identical σ values despite the water content of the latter being 30 times

greater than the former. This data can be explained by taking into account the relationship between conductivity and water content, as shown in Equation 2:

$$\sigma_{X^-} = F[X^-]\mu'_{X^-} \quad (2)$$

where F = Faraday's constant, μ'_{X^-} = effective anionic mobility (which accounts for both the association strength between cationic sites and X^-, and the tortuosity of the ionic path) and $[X^-]$ = analytical anion concentration (calculated values are listed in Table 2).[63-64] For example, the high water content of the Cl^- membrane (λ = 167) facilitates ion transport and leads to a considerably greater mobility compared to other membranes; however, the larger water content causes $[X^-]$ to be much lower, which results in similar conductivity values for the Cl^- and HCO_3^- membranes.

The μ'_{X^-} values for all the membranes except Cl^- are approximately 1 to 2 orders of magnitude lower than the mobility of free anions at infinite dilution in aqueous solutions ($\mu_{X^-}^{\infty}$, listed in Table 2).[65] This is likely due to their low water content, as discussed above. In PEMs, it has been found that the complete separation of the proton and fixed anion does not fully occur unless λ ≥ 6.[66] For similar λ values (3–6), the effective proton mobility in Nafion® and sulfonated α-β-β-trifluorostyrene-based BAM® membranes is also 1 to 2 orders of magnitude lower than free protons at infinite dilution (3.62×10^{-3} cm^2 V^{-1} s^{-1}).[63,67] It is likely that the amount of solvent molecules present at low λ are inadequate for full ion pair separation in these AEMs.

An interesting observation is that the infinite mobility values for the anions are within 10% of each other (except for Cl^-), but they show significant variation in the μ'_{X^-} values as a function of X^-. In Nafion® and BAM® membranes, mobility differences can be attributed to their different morphological structures, but all of the AEMs studied have the same backbone. It is therefore apparent that the interaction of X^- with the polymer backbone plays a role in determining the anion mobility. Regarding the Cl^- membrane, the high λ value allows for the anions to more easily be solvated and separated from the fixed cations, which explains why its μ'_{X^-} value is much closer to the mobility of Cl^- solutions at infinite dilution.

A recent paper by Yan and Hickner reported the conductivity of HCO_3^- in AEMs based on quaternary ammonium-substituted poly(aryl ethersulfone).[68] The maximum observed conductivity was 2.73 x 10^{-2} S cm^{-1}) for a membrane with an IEC of 2.09 meq g^{-1}. P(DMBI)-HCO_3^- showed a lower conductivity than Yan and Hickner's AEM, but also had a much lower water content (λ = 5 vs. 44).

The triiodide (I_3^-) conductivity of P(DMBI) in the solid state was also investigated, since this polymer has the potential to be used as a solid electrolyte in DSSCs. Samples of P(DMBI)-I^- were soaked in an I_2-saturated methanol (MeOH) solution and air dried for 24 h. The estimated iodine uptake was 1.4 moles of I_2 per mole of I^- originally present. Interestingly enough, P(DMBI)-I_3^- membranes possessed even lower water content than the parent P(DMBI)-I^- membranes but exhibited a similar (wet) conductivity value (2.7 x 10^{-3} S cm^{-1} for the former, 3.3 x 10^{-3} S cm^{-1} for the latter). Dry samples of P(DMBI)-I_3^- exhibited a conductivity of 5.0 x 10^{-4} S cm^{-1} which is comparable to previously reported values of 5.0 x 10^{-4} S cm^{-1} and 8.0 x 10^{-4} S cm^{-1} for polyphosphazene[69] and poly(ethylene oxide)/ poly(vinylidene fluoride)-based[70] solid electrolytes, respectively, that have been used in DSSCs.

Conductivity measurements at different temperatures and relative humidity values were also done for X^- = I^-, Br^- and Cl^- (data shown in Figures 2.8, 2.911 and 2.10, respectively). All three membranes showed the same trend for all temperatures in which their conductivity was consistently low (<0.5 mS cm^{-1}) until the relative humidity (RH) reached 95%, whereupon an increase in conductivity was seen. The iodide membrane had the most dramatic increase in σ_{max} with temperature, going from ~5 mS cm^{-1} at 30°C up to ~47 mS cm^{-1} at 50°C. The chloride membrane also showed an increase in σ_{max} with temperature, going from ~1 mS cm^{-1} at 30°C up to ~30 mS cm^{-1} at 50°C. The bromide membrane did not display a trend in σ_{max} with respect to temperature, as σ_{max} increased from 40°C < 50°C< 30°C. Also, it shows a very small increase in conductivity compared to the other two membranes, as it only goes from 0.45 mS cm^{-1} at 40°C to ~1.8 mS cm^{-1} at 30°C.

It is expected that the conductivity would increase with increasing ionic radius due to a larger free volume for conduction[71], as this behaviour has been observed in similar polymers[72-73]; however, this is not the case with the bromide membrane. Since

these measurements were done on the same membrane three times, it cannot be a methodical error. There is potentially a different morphology in this membrane, but as studies of this membrane were not the primary aim of this thesis, this was not investigated further.

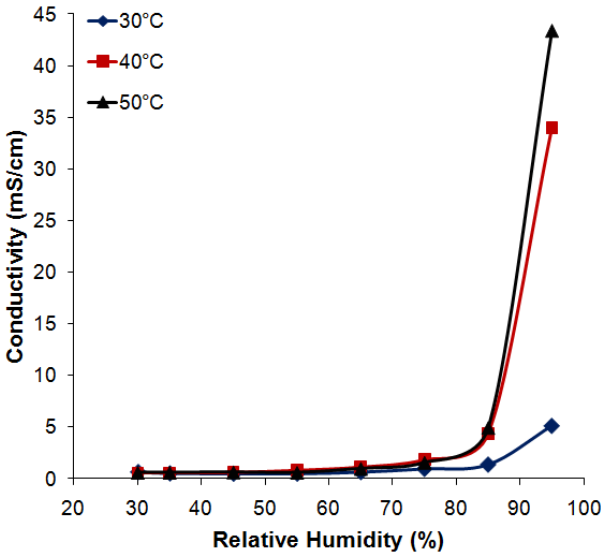

Figure 2.8: Conductivity vs. relative humidity plot for P(DMBI)-I^- at different temperatures.

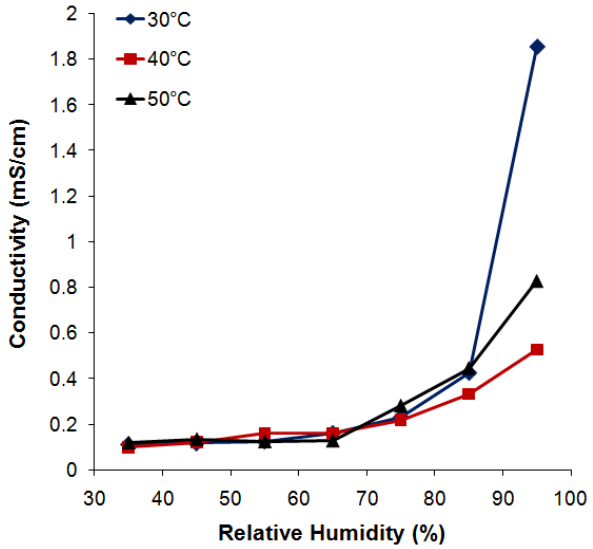

Figure 2.9: Conductivity vs. relative humidity plot for P(DMBI)-Br^- at different temperatures.

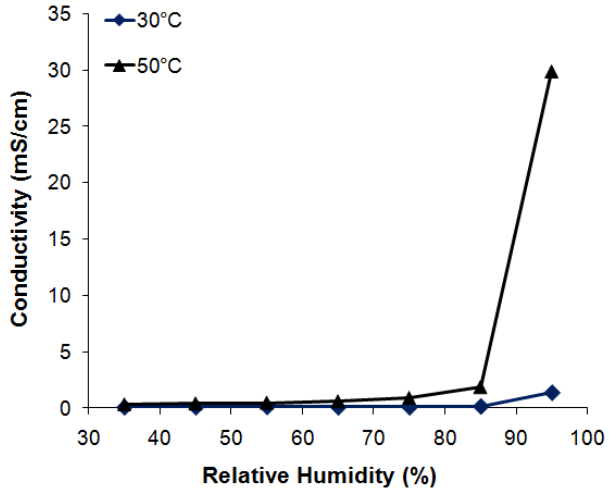

Figure 2.10: Conductivity vs. relative humidity for P(DMBI)-Cl^- at different temperatures.

2.5. Conclusion and Future Work

The polymer P(DMBI)-I^- was found to be stable and a good anion conductor. Studies on this and other anionic forms of this polymer showed that both water uptake and conductivity were anion-dependent. P(DMBI)-I^- was also converted to the triiodide form and shown to have a conductivity on par with electrolytes used in DSSCs, which makes it a promising candidate for this use.

Future experiments can be done in which PBI is alkylated with other R-groups such as ethyl or phenyl in order to stabilize it in the hydroxide forms. It would also be interesting to compare the conductivity and water uptake values with those presented above to further investigate the backbone-anion interaction.

Further investigations can also be made into the effect of temperature on the conductivity of these membranes. Comparisons of λ values at elevated temperatures as well as Dynamic Vapour Sorption (DVS) measurements of water uptake at different temperatures could also be done to determine the effect of temperature on λ. Experiments to examine the morphology of the polymers, such as TEM or AFM, could also be investigated to learn more about the factors that affect the polymer's conductivity,

In order to deduce the exact nature of the polymers' decomposition products, the TGA experiments could be repeated with the TGA analyzer coupled to a mass spectrometer.

2.6. Experimental

2.6.1. Synthesis

2.6.1.1. Materials

All chemicals were obtained from Sigma-Aldrich Canada Ltd. unless stated otherwise. Deionized H_2O was purified using a Millipore Gradient Milli-Q® water purification system. All chemicals were used as-is except for 3,3'-diaminobenzidine and isophthalic acid, which were purified according to literature procedures.[74]

2.6.1.2. Synthesis of PBI

PBI was produced according to literature procedures to produce a high molecular weight polymer[46]. A typical procedure is described here: 3,3'-diaminobenzidine (9.3450 g, 43.6 mmol) was dissolved in 300 g polyphosphoric acid at 140°C. Isophthalic acid (7.246 g, 43.6 mmol) was slowly added and the solution heated to 180°C overnight, and then slowly poured into 3 L of water to precipitate the polymer. Sodium carbonate was added to this solution until it was basic, and the solution was stirred overnight to neutralize residual phosphoric acid. The polymer was then dried overnight at 80°C, ground to a powder using liquid nitrogen, then dried again overnight. Yield: 14.5 g (98%) (47 mmol).

^{1}H NMR (500 Hz, DMSO-d_6, δ, ppm): 13.30 (2H, s, H_G), 9.18 (1H, s, H_D), 8.35 (2H, d, 1 Hz, H_E), 8.06 (1H, s, H_F), 7.70 (6H, m, $H_{A,B,C}$).

2.6.1.3. Synthesis of P(DMBI)-I^-

P(DMBI)-I^- was made based on a literature procedure[40] and a typical synthesis is described here. PBI (10 g, 32 mmol) was dissolved in anhydrous NMP (450 mL) under argon at 100°C, then cooled to room temperature. LiH (0.6364 g, 80 mmol) was then slowly added, and then the temperature was increased to 100°C and stirred for 15 h. The solution was cooled to room temperature and iodomethane (excess, 100 g, 704 mmol) was added, and then the temperature was raised to 60°C for 6 hours. The resulting light brown precipitate was separated from the solution using vacuum filtration, and then dissolved in DMSO (500 mL) before addition of 114 g (803 mmol) of iodomethane. The mixture was heated to 90°C for 15 hours, and the polymer precipitated in 1.5 L of stirring water. The resulting brown solid was vacuum filtered and residual DMSO was removed using Soxhlet purification with acetone for 24 hours. Yield: 8 g (80%) (12.8 mmol).)

^{1}H NMR (500 Hz, DMSO-d_6, δ, ppm): 8.84−8.26 (10H, aromatic protons, H_{A-E}), 4.23, 4.15 (11.89H, methyl protons $H_{G,H}$).

2.6.2. Instrumentation

2.6.2.1. Nuclear Magnetic Resonance (NMR)

^{1}H NMR spectra were obtained using a Varian Unity Spectrometer operating at 400 MHz. The polymers were dissolved in DMSO-d_6 at a concentration of approximately 30 mg mL^{-1}.

2.6.2.2. Fourier Transform Infrared Spectroscopy (FTIR)

Fourier transform infrared spectroscopy (FTIR) was performed on a Bomem FTLA2000-154 FTIR system. Polymer films were drop-cast from a dilute DMSO solution onto a glass slide and dried under vacuum at 80 °C for 2 h prior to experiments.

2.6.2.3. Thermal Gravimetric Analysis (TGA)

TGA data were obtained using a TGA-50 Shimadzu Thermogravimetric analyzer. Each run was performed under nitrogen gas at a heating rate of 10°C/minute with a sample size between 10-20 mg.

2.6.3. Characterization Procedures

2.6.3.1. Preparation of P(DMBI)-I^- Membranes.

Membranes of P(DMBI)-I^- were cast from 0.02 g mL^{-1} DMSO solutions onto flat Petri dishes, heated to 80°C overnight in air and dried under vacuum at 50°C for 2 h.

2.6.3.2. Preparation of P(DMBI)-X^- Membranes through Ion Exchange

Ion exchange was done through immersion of P(DMBI)-I^- membranes in 1 M solutions containing the potassium salt of the desired anion for 24 hours (e.g. to get the chloride form, the membrane was soaked in 1 M $KCl_{(aq)}$). For consistency, the initial P(DMBI)-I^- was also soaked in a 1 M $KI_{(aq)}$ solution even though it was already in the iodide form. After conversion, membranes were washed repeatedly with deionized water to remove any remaining salt solution.

2.6.3.3. Anion Conductivity Measurements

Conductivity data were obtained using AC impedance spectroscopy with a Solartron 1260 frequency response analyzer. Membranes were cut to dimensions of

approximately 0.5 cm x 1.5 cm and then soaked in deionized water overnight prior to experimental measurements. These were laid across two platinum electrodes (0.5 x 1cm) set 0.5 cm apart that were adhered to a PTFE block. Another block was placed on top and the assembly held together by clips during the measurement period. Both blocks had rectangular holes on top and bottom so that membranes could remain hydrated. The membranes' dimensions were measured using a calliper (length and width, ± 0.1 mm) and a micrometer (thickness, ± 0.001 mm).

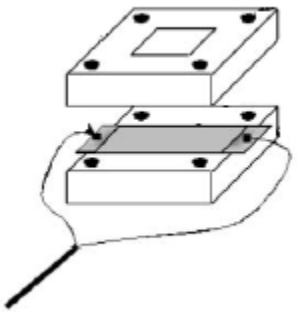

Figure 2.11: A schematic diagram of the assembly used for impedance measurements. The gray section represents the membrane.[64]

Two wired alligator clips were used to connect the PTFE apparatus with the frequency response analyzer. A 100 mV sinusoidal AC voltage was then applied between the two platinum electrodes between the frequencies of 10 MHz – 100 Hz and then the AC resistance, i.e. the impedance, was measured. Measurements were collected several times over twenty minutes or until a constant ionic resistance was obtained, and then measured in triplicate. Data was analyzed using ZPlot software from Scribner.

The ionic resistance, R_m was calculated from the impedance data and fitted to an equivalent standard Randles circuit model using non-linear least squares regression. The anion conductivity, σ_{X^-} was then calculated from the resistance using Equation 3 below:

$$\sigma_{X^-} = \frac{L}{R_m A} \quad (3)$$

where L is the distance length between the platinum electrodes and A is the cross-sectional area of the membrane (width x height).

Conductivity measurements performed with different relative humidity and temperature values were regulated using an Espec humidity chamber.

2.6.3.4. Ion Exchange Capacity (IEC) measurements

IEC measurements were obtained by immersing the membranes overnight in a 1 M $NaNO_{3(aq)}$ solution to release the X^- anion, and then titrating the solution with 0.1 M $AgNO_{3(aq)}$ using 10% $K_2CrO_{4(aq)}$ as an indicator. The IEC was calculated as follows:

$$IEC = \frac{moles\ of\ X^-}{mass\ of\ dry\ membrane}$$

2.6.3.5. Volume and Water Uptake Measurements

These measurements were achieved by first weighing and measuring the dry membranes, then immersing them in the desired solvent for 24 hours. The wet membranes were placed between two glass slides when measuring their area in order to prevent them from drying out during the measurement time. Their wet masses were determined by quickly blotting them with Kim Wipes to remove surface water and then weighing them.

3. Mesitylene-Poly(dimethylbenzimidazolium) – A Novel Anion Exchange Membrane

The majority of this section is reprinted from:

Owen D. Thomas, Kristen J. W. Y. Soo, Timothy J. Peckham, Mahesh P. Kulkarni, Steven Holdcroft, A Stable Hydroxide-Conducting Polymer. *Journal of the American Chemical Society*, **2012**, 134(26), 10753-10756.

3.1. Contributions

Owen Thomas synthesized the mesitylene dicarboxylic acid. Owen Thomas and Mahesh Kulkarni synthesized Mes-PBI. I synthesized Mes-P(DMBI)-I^- with their help. I cast all the membranes, performed all NMR analyses, anion exchange conversions, and conductivity measurements. I edited all drafts of the manuscript. Graeme Suppes did the computational modelling calculations. Dev Sharma did all of the TGA measurements. Dr. Khalid Fatih performed the fuel cell experiments.

All of the contents of this chapter were reported in the paper except for the following: Section 3.4.2 up until and including Table 3; Table 4, Figure 3.17, Figure 3.19, Table 6, and Figures 3.20 – 3.23 and all observations and discussion associated with the aforementioned tables and figures in Section 3.4.3.

3.2. Introduction to Blend Membranes

PBIs have been used in the cross-linking of PEMs to make blend membranes, as they confer mechanical and thermal stability to high-IEC polymers that swell greatly in water. In doing so, though, they also decrease the IEC of the resulting membrane, owing to the formation of ionic cross-links between the basic nitrogen on PBI and the acidic

proton on the PEM. This has the effect of decreasing the blend membranes' conductivity, as the IEC is lowered, and so efforts have been made to find optimal ratios between PBI and the PEM for a high-performance membrane,[75-76]Interestingly enough, PBI has not been used in this manner to crosslink anion-exchange membranes, and so this section of the thesis describes our pioneering work in this area.

As briefly described in Section 2.4.3, it was found that the P(DMBI)-OH^- membrane was not mechanically stable. Stability tests on small molecule analogues of the polymer were done by Owen Thomas, which showed that the polymer was likely degrading due to imidazole ring opening by nucleophilic hydroxide attack, as shown in Figure 3.1. It was also found that a small molecule analogue possessing propyl groups on the nitrogen atoms instead of methyl groups was stable over many hours, and did not display hydroxide attack. Synthesis of the analogous polymer proved unsuccessful, but based on these results, it was inferred that the presence of bulkier groups around the positively charged imidazolium carbon would protect it from being attacked by the hydroxide ion, thus allowing it to be a hydroxide conductor.[77]

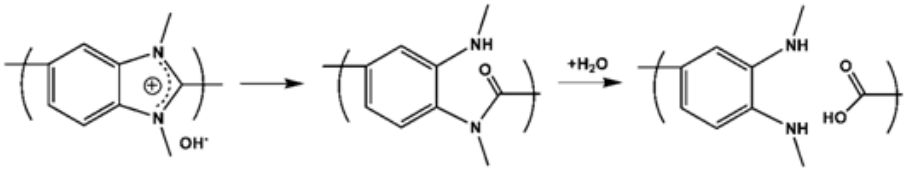

Figure 3.1: Hydroxide attack on the small molecule analogue of P(DMBI)-OH^-, showing Hofmann elimination at the C2 carbon.

With this knowledge, another modified form of P(DMBI)-I^- was proposed as a stable, hydroxide-conducting polymer. This modified form, shown below in Figure 3.2, is called mesitylene-P(DMBI)-I^-, hereafter known as Mes-P(DMBI)-I^-. Instead of adding the bulkier groups to the imidazolium ring, three methyl groups were added to the phenyl ring in the polymer, making it a mesitylene group. Computational calculations predicted that there would be ring twisting in Mes-P(DMBI)-I^- that would allow for two of the mesitylene methyl groups to sit above and below the C2 carbon, thereby providing a means of protection against hydroxide attack in Mes-P(DMBI)-OH^-. It was also predicted that the C2 carbon would be exposed to hydroxide attack in P(DMBI)-I^-, as there were no bulky

groups to protect it. The space-filling models of P(DMBI)-I^- and Mes-P(DMBI)-I^- as found from those calculations are shown in Figure 3.3a and b, respectively.[78] If this polymer could be synthesized and found to be stable, it would represent the first known stable hydroxide-conducting polymer.

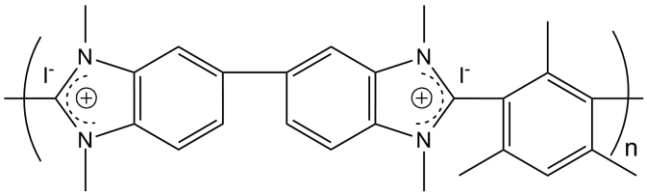

Figure 3.2: The novel polymer Mes-P(DMBI)-I^-.

Figure 3.3: Space-filling models of (a) P(DMBI)-I- and (b) Mes-P(DMBI)-I-.

Synthesis of Mes-P(DMBI)-I^- from a tetraamine and a mesitylene dicarboxylic acid was successful, as described in Section 3.6.1.4, and tests on its bromide and chloride forms were done as described in Section 3.4.3. However, this polymer was found to dissolve upon addition to a hydroxide solution, and while this allowed for stability tests through ^{1}H NMR spectroscopy, this solubility limits its application as an anion exchange membrane.

A strategy of polymer blending was therefore developed to prevent dissolution that utilized the ability of PBIs to be converted into cationic and anionic forms. Membranes were prepared from blends of Mes-P(DMBI)-I^- with controlled amounts of the novel, neutral polymer, mesitylene-polybenzimidazole (Mes-PBI), whose structure is shown in Figure 3.4. Immersing these blend membranes in a $KOH_{(aq)}$ solution removed the weakly acidic N−H protons in Mes-PBI, which rendered the ring negatively charged

(Figure 3.4) and independently but simultaneously converted Mes-P(DMBI)-I^- to Mes-P(DMBI)-OH^-. The films were washed to remove excess $KOH_{(aq)}$ and then rendered insoluble by virtue of the ionic interaction between the negatively charged benzimidazolide and positively charged benzimidazolium rings.[78]

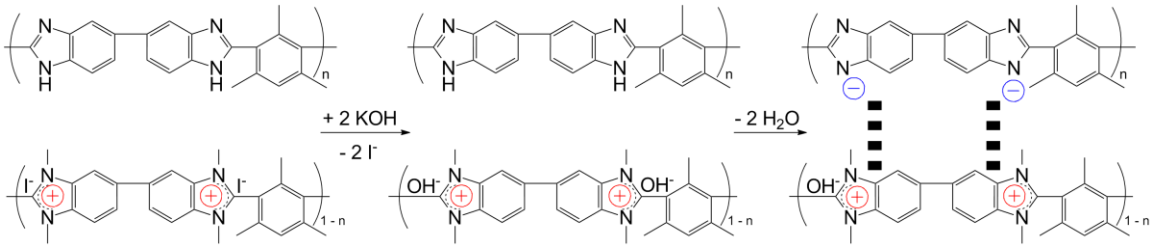

Figure 3.4: Scheme for the formation of blend membranes of Mes-PBI and Mes-P(DMBI)-OH^-.

3.3. Materials Used

3.3.1. Mes-PBI

Mes-PBI is a novel polymer that was synthesized from the condensation of 3,3'-diaminobenzidine and a mesitylene dicarboxylic acid. Its structure is shown below in Figure 3.5.

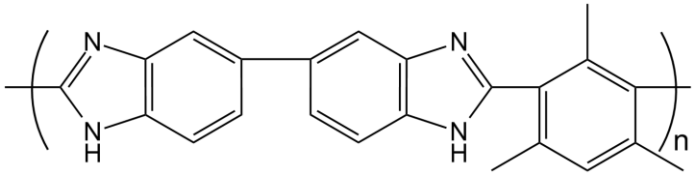

Figure 3.5: Structure of the polymer mesitylene-polybenzimidazole (Mes-PBI).

3.3.2. Mes-P(DMBI)-X^-

Mes-P(DMBI)-X^- is also a novel polymer that was synthesized in the iodide form through a two-step reaction in which Mes-PBI was delithiated and then alkylated with methyl iodide. Its structure is shown below in Figure 3.6.

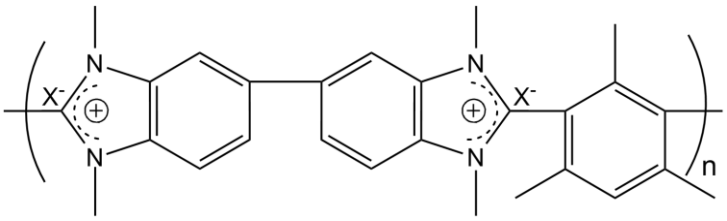

Figure 3.6: Structure of the polymer mesitylene-poly(dimethylbenzimidazolium) (Mes-P(DMBI)-X$^-$).

3.3.3. Blends of Mes-PBI and Mes-P(DMBI)-OH$^-$

Blends of Mes-PBI and Mes-P(DMBI)-OH$^-$ were synthesized by casting membranes of controlled amounts of Mes-PBI and Mes-P(DMBI)-I$^-$ in DMSO, then immersing the membranes in 0.5 M $KOH_{(aq)}$ to convert them to the hydroxide form and also create ionic cross-links to ensure its insolubility in water. The general structure of a blend membrane is shown below in Figure 3.7.

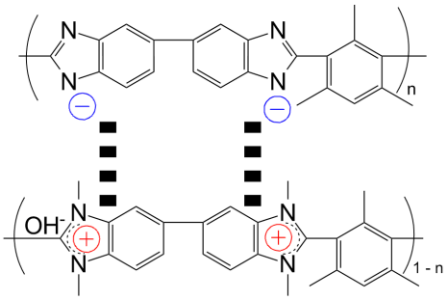

Figure 3.7: General structure of a blend membrane of Mes-PBI and Mes-P(DMBI)-OH$^-$.

3.4. Results and Discussion

3.4.1. Polymer Synthesis and Basic Analysis

The dicarboxylic acid was produced following the scheme shown below in Figure 3.8.[79-80]

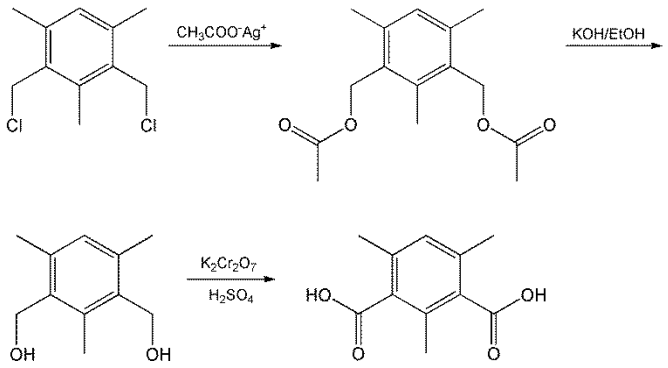

Figure 3.8: Scheme showing the synthesis of the mesitylene dicarboxylic acid monomer.

Mes-PBI was produced using the same synthesis scheme as Iwakura et al,[46] except using the mesitylene dicarboxylic acid shown above.

Mes-P(DMBI)-I^- was produced following the synthesis scheme outlined by Hu et al. for P(DMBI)-I^-, but using Mes-PBI as the starting polymer instead.[40]

The ^1H NMR spectra of Mes-PBI and Mes-P(DMBI)-I^- are shown below in Figures 3.9 and 3.10, respectively. For Mes-PBI, there are three singlets at 7.97, 7.76 and 7.25 ppm and a multiplet at 7.25 ppm. Their relative integrations add to 7.4, which is close to the theoretical number of 7 aromatic protons. There is also a multiplet at 12.71 ppm that has a relative integration of 2.00. Lastly, the two singlets at 2.18 and 1.92 ppm integrate to relative intensities of 6.19 and 3.15 for a total of 9.34 protons where 9 are expected. This gives reasonable evidence that this polymer was synthesized successfully, and the only other peaks that are present are solvent peaks (H_2O at 3.35 ppm and DMSO at 2.51 ppm).

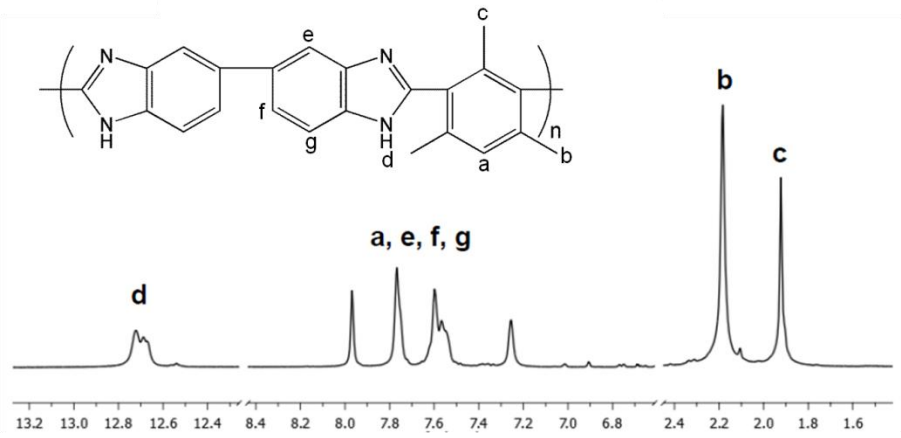

Figure 3.9: ^{1}H NMR spectrum of Mes-PBI.

Figure 3.10: ^{1}H NMR spectrum of Mes-P(DMBI)-I^{-}.

The ^{1}H NMR spectrum of Mes-P(DMBI)-I^{-} shows three singlets in the aromatic region at 8.81, 8.41 and 7.82 ppm, which integrate to 2, 4 and 1 protons respectively. These three peaks correspond to the seven protons that are attached to the three benzene groups in the polymer backbone. This is one less singlet than the P(DMBI)-I^{-} polymer, which is due to the replacement of protons by methyl groups on the benzene ring. In the alkyl region of the NMR spectrum, there are four singlets (excluding solvent peaks) at 4.13, 4.06, 2.30, and 2.00 ppm. The two singlets at 4.13 and 4.06 ppm integrate together to 12 protons, and these are the methyl protons attached to the

nitrogen atoms on the imidazolium group. This assignment was made based on the fact that these singlets appear at nearly identical chemical shift values in the P(DMBI)-I^- spectrum. The other two singlets integrate to 6 and 3 protons respectively, which are the nine methyl protons attached to the phenyl ring. The fact that the proton integration values and chemical shifts have the expected values confirm that the product is the desired polymer, and the lack of other peaks apart from water (3.35 ppm) and DMSO (2.50 ppm) confirms its purity.

3.4.2. Mes-P(DMBI)-X^- Properties

Mes-P(DMBI)-I^- polymer was found to swell much more than P(DMBI)-I^- in water, which is likely due to the fact that the polymer chains are now unable to pack together as tightly due to the extra methyl groups on the benzene ring in the polymer backbone. This high swelling is also a likely contributor to its relatively high conductivity when wet, as this allows for more water molecules to solvate the anions and allow them to conduct.

Mes-P(DMBI)-I^- was converted to the bromide and chloride forms using ion exchange as described in Section 2.4.3, and the membranes swelled noticeably and became very thin, and then broke apart when washed gently with water. The membrane pieces were then dried overnight and re-cast in DMSO for analysis. The chloride membrane swelled so much that it broke apart as soon as it was taken out of water, and repeated experiments confirmed its mechanical instability, so no water uptake or conductivity measurements could be obtained. A full water uptake comparison can be seen in Table 3, where it is evident that the addition of the mesitylene group caused all of the Mes-P(DMBI)-X^- polymers to swell more, likely due to the increase in free volume in the polymer. The conductivity values, as seen in Table 4, are also higher for the Mes-P(DMBI)-X^- polymers, which is likely due to an increase in anion mobility from the higher water content.

Table 3: Water uptake comparison of P(DMBI)-X^- and Mes-P(DMBI)-X^-.

Polymer	Water Uptake (%)
P(DMBI)-I^-	10 ± 2
Mes-P(DMBI)-I^-	152 ± 8
P(DMBI)-Br^-	12 ± 1
Mes-P(DMBI)-Br^-	82 ± 6
P(DMBI)-Cl^-	1920 ± 80
Mes-P(DMBI)-Cl^-	n/a

Table 4: Wet conductivity comparison of P(DMBI)-X^- and Mes-P(DMBI)-X^-.

Polymer	Conductivity (mS cm^{-1})
P(DMBI)-I^-	3.3 ± 0.4
Mes-P(DMBI)-I^-	6 ± 0.3
P(DMBI)-Br^-	3.2 ± 0.4
Mes-P(DMBI)-Br^-	9.9 ± 0.4
P(DMBI)-Cl^-	7.6 ± 1.1

TGA measurements were performed on Mes-P(DMBI)-I^-, Mes-P(DMBI)-Br^-, Mes-P(DMBI)-Cl^-, and Mes-P(DMBI)-OH^-, and these curves are shown in Figure 3.11. Mes-P(DMBI)-I^- loses ~10% of its mass up to 110°C, and is then stable until 232°C, where it loses ~18% of its mass up to 326°C and then decomposes past 414°C. Mes-P(DMBI)-Br^- lost ~5% of its mass before 55°C and then remained stable until 163°C, where it lost 40% of its mass up to 346°C and then remains stable until it begins to decompose at 540°C. Mes-P(DMBI)-Cl^- loses 6% of its mass before 71°C, then remains stable until 159°C where it then loses 35% of its mass up to 375°C and then remains stable until it begins to decompose at 506°C. Mes-P(DMBI)-OH^- lost 14% of its mass by 85°C and was stable up to 200°C, where it then lost 5% of its mass by 337°C and then another 20% of its mass by 398°C. It decomposed past this temperature.

Overall, it can be seen that the Mes-P(DMBI)-X^- display similar TGA curves to their corresponding P(DMBI)-X^- polymers, in that they show one major decomposition past 100°C and then gradually decompose. The Mes-P(DMBI)-X^- polymers all begin to decompose at a lower temperature than the analogous P(DMBI)-X^- polymer, with the

exception of the iodide form. Also, none of them seem to decompose through the loss of the methyl halide (or methanol in the case of the hydroxide form), which suggests that they undergo a different decomposition mechanism than their non-mesitylene analogues. It is possible that some sort of other compounds with the halide/hydroxide anion may be forming, and at higher temperatures, it is expected that they would show similar decomposition products to their P(DMBI)-X^- analogues (i.e. ammonia, hydrogen cyanide, nitrogen, and condensed heterocyclic species;[52-53] however, as stated in Section 2.4.3, determining the exact nature of these products was not the focus of this thesis, as the purpose of the TGA experiments was to determine the thermal stability of these compounds.

The TGA results are summarized in Table 5.

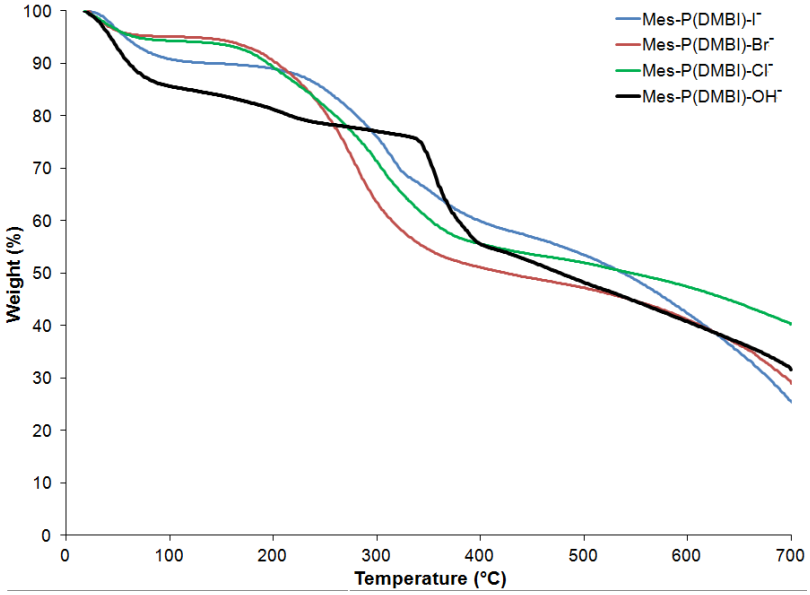

Figure 3.11: TGA plots for Mes-P(DMBI)-I^- (blue curve), Mes-P(DMBI)-Br^- (red curve), Mes-P(DMBI)-Cl^- (green curve) and Mes-P(DMBI)-OH^- (black curve)

Table 5: Table summarizing the TGA data for P(DMBI)-X^- and Mes-P(DMBI)-X^-.

Polymer	Highest Stable Temperature (°C)
P(DMBI)-I^-	160
Mes-P(DMBI)-I^-	232
P(DMBI)-Br^-	216
Mes-P(DMBI)-Br^-	163
P(DMBI)-Cl^-	212
Mes-P(DMBI)-Cl^-	159
Mes-P(DMBI)-OH^-	200

.A film of Mes-P(DMBI)-I^- was found to dissolve in 0.1 M $KOH_{(aq)}$. Upon dialysis and removal of water by rotary evaporation, a thin yellow-brown film of Mes-P(DMBI)-OH^- was formed. Conductivity values for this membrane in both the iodide and hydroxide forms at room temperature and non-humidified air are shown in Table 6, and they were found to be nearly identical within equipment and experimental error.

Table 6: Dry conductivity values of Mes-P(DMBI)-I^- and Mes-P(DMBI)-OH^-.

Polymer	Conductivity (mS cm^{-1})
Mes-P(DMBI)-I^-	0.3 ± 0.2
Mes-P(DMBI)-OH^-	0.4 ± 0.2

In order to investigate the stability of Mes-P(DMBI)-OH^- over time, this polymer was dissolved in a solution of 0.5 M $KOH_{(aq)}$ in D_2O and ^1H NMR measurements were taken over thirty days at room temperature, as shown in Figure 3.12.

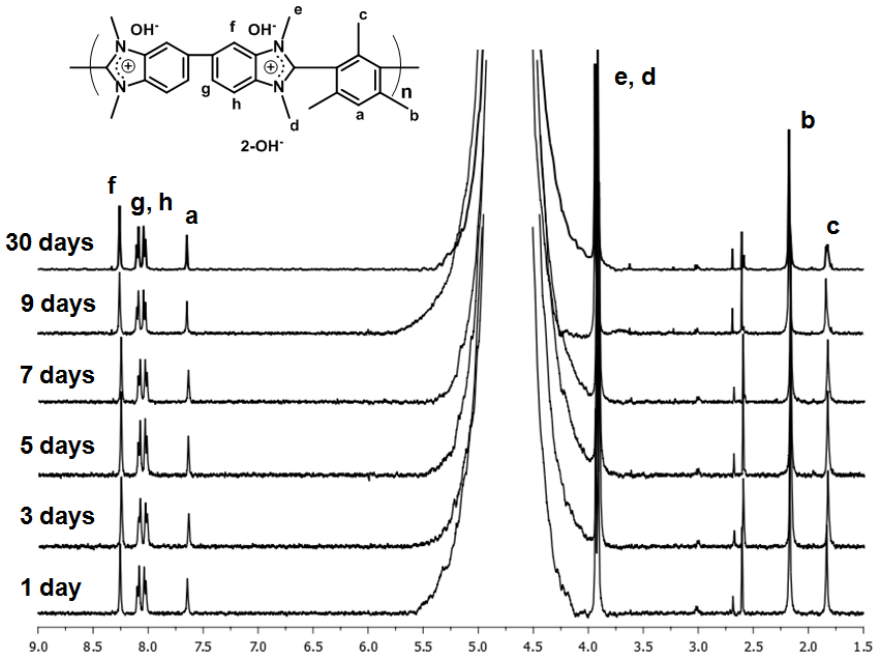

Figure 3.12: ^1H NMR spectra of Mes-P(DMBI)-OH^- over 30 days at room temperature in 0.5 M $KOH_{(aq)}$.

This NMR experiment was repeated using 2 M $KOH_{(aq)}$ and heating the solution to 60°C over a period of 10 days in order to see if the elevated temperature would affect the polymer's stability. The resulting spectra are shown in Figure 3.13. It was found that deuterium exchange affected the peak height of some of the signals. This exchange is common under prolonged exposure to deuterated solvents particularly in the presence of base,[81-82] as is the case in this study. The peak integrals lost due to deuterium exchange are peaks B, C, F and H. The stability of the polymer was ascertained by integrating the peaks not prone to deuterium exchange (i.e., peaks G, A, E and D) at the end of 10 days, and they were found to maintain the same ratios as the starting polymer. In addition, no new peaks were formed over the time period of this experiment, so the stability of the polymer is unmistakable.

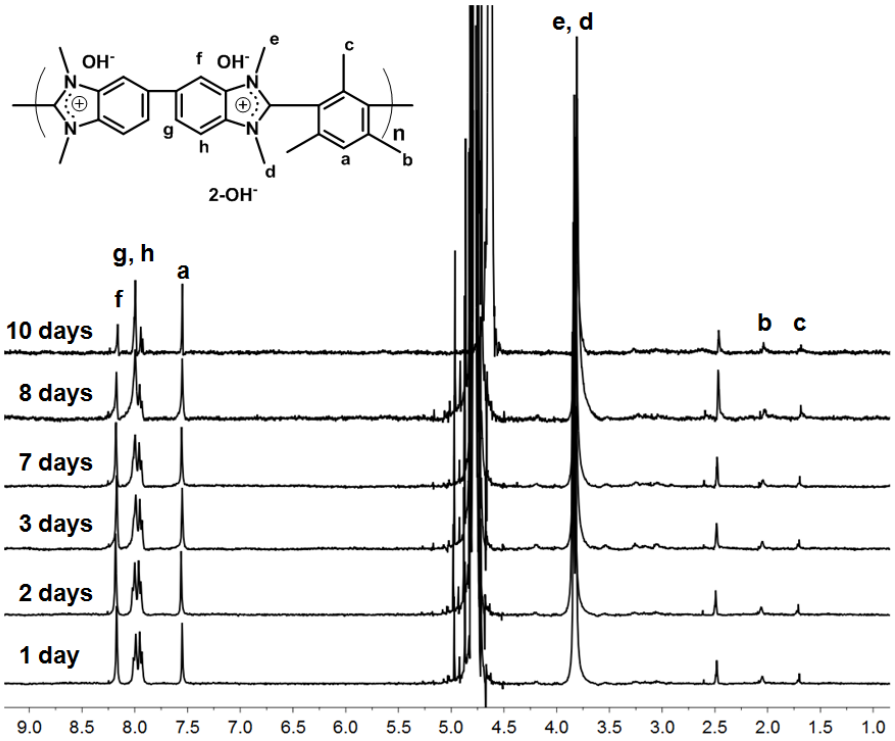

Figure 3.13: ^{1}H NMR spectra of Mes-P(DMBI)-OH- over 10 days at 60°C in 2 M $KOH_{(aq)}$.

The dissolution of Mes-P(DMBI)-OH^- polymer in $KOH_{(aq)}$ prevented it from being tested for use as an anion exchange membrane, and so Section 3.4.4 details work that was done to mechanically stabilize this polymer in aqueous solution.

3.4.3. Blend Membrane Properties

Blend membranes of controlled amounts of Mes-PBI and Mes-P(DMBI)-OH^- were synthesized to investigate whether or not the presence of Mes-PBI would mechanically stabilize Mes-P(DMBI)-OH^- in water. A full series of blend membranes were made with theoretical IEC values (in the hydroxide form) of 2.5, 2.0, 1.5 and 1.0.

Blend membranes were made by mixing the appropriate amounts of DMSO solutions of Mes-PBI and Mes-P(DMBI)-I^- together, then casting films and immersing them in $KOH_{(aq)}$ to convert them to the hydroxide form. Representative calculations for this can be found in the appendix. The titrated IEC values obtained were 98% of the

expected values, which means that the ion exchange from the iodide form to the hydroxide form is very effective.

The water uptake and wet conductivity values for the blends in the iodide and hydroxide forms are shown in Tables 7 and 8, respectively, as well as their λ values. The errors in the table represent equipment error. The experimental values measured by back-titration matched the theoretical values calculated. For both blend series, the λ values increased with increasing IEC, and the conductivity was found to mostly scale with increasing IEC. The blend membrane in the iodide form with an IEC of 2.59 was found to have broken apart some time during the conductivity measurements, which is likely why the conductivity measurement was so low. This is likely due to swelling. For the blend membranes in the hydroxide form, it was a bit surprising to see that the conductivity with an IEC of 2.0 was lower than that for 1.5, especially given the higher λ value, but it is likely that the high water uptake caused the anion concentration to be diluted, thus somewhat negating the higher IEC and accounting for the lower conductivity value.

Table 7: Properties of blends of Mes-PBI and Mes-P(DMBI)-I^-.

Blend IEC (I^-)	Mass Uptake of Water (%)	λ	Conductivity (mS cm^{-1})
2.23	18 ± 5	4	3.59 ± 0.09
2.35	44 ± 6	10	5.99 ± 0.06
2.47	51 ± 5	12	7.37 ± 0.06
2.59	112 ± 8	24	0.58 ± 0.09

Table 8: Properties of blends of Mes-PBI and Mes-P(DMBI)-OH^-.

Blend IEC (OH^-)	Mass Uptake of Water (%)	λ	Conductivity (mS/cm)
1.0	82 ± 5	23	9.6 ± 0.1
1.5	119 ± 4	33	10.1 ± 0.1
2.0	162 ± 9	45	13.2 ± 0.1

All of the blend polymers were found to have a lower water uptake in the iodide form than Mes-P(DMBI)-I^-, which is undoubtedly due to the mechanical stability afforded to them by Mes-PBI. The hydroxide polymers also have a generally higher water uptake than the iodide membranes, which likely contributes to their conductivities also being higher. The increased water content likely allows for easier ion solvation and transport through the membrane.

The hydroxide stability of the blend membranes over time at room temperature was measured by performing conductivity measurements each day for ten days straight in a fully humidified environment, as seen below in Figure 3.14, and it was found that their conductivity values did not change by more than 15% over the experimental time period, indicating relative stability. The conductivity values are lower than those reported in Table 6 because a newer, more accurate conductivity apparatus was used to measure them, as described in Section 3.6.3.1.

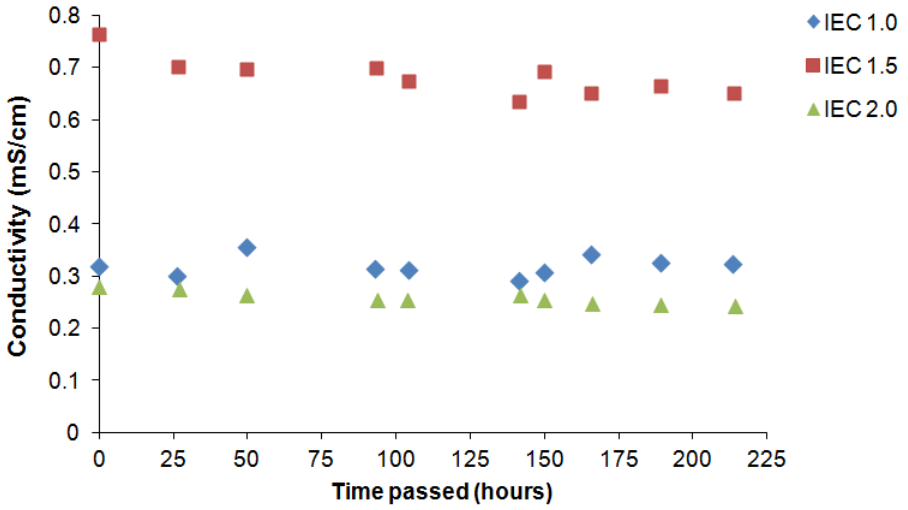

Figure 3.14: Hydroxide conductivity of the blend membranes over time at room temperature in fully humidified air.

The hydroxide stability of these blends was examined by monitoring the change in IEC over time for membranes soaked in 2 M $KOH_{(aq)}$ at 60 °C. The membranes with an IEC of 1.5 were stable to within 5% of the original value after 13 days, as seen in Figure 3.15.

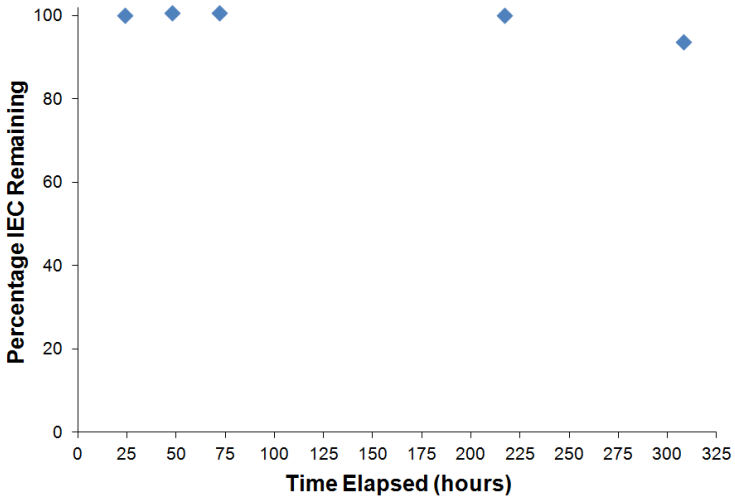

Figure 3.15: Change in IEC over time for blend membrane soaked in 2 M $KOH_{(aq)}$ at 60°C over 13 days.

The chemical stability and reversibility of the ionic cross-linking was also tested by immersing the membranes in 2 M $HCl_{(aq)}$ to convert them to the chloride form, and then an attempt was made to dissolve them in DMSO. The membranes were found to be sparingly soluble in DMSO, indicating that the cross-linking is only marginally reversible.

The conductivity range of the blend membranes was between 9−13 mS cm^{-1}. This is in keeping with typical anion conductivities in hydrated membranes found in the literature, such as quaternary ammonium-substituted poly(aryl ether sulfone),[68] Nafion-based anion-exchange membranes,[23,83] and ionic-liquid-derived membranes,[84-85] but lower than those of the poly(phenylene)- based polymers described by Hibbs et al.[86] It is noted that the conductivity decreased with increasing IEC, which is common for membranes with high ion content, where excessive swelling and subsequent ion dilution lowers the conductivity.[87]

Two blend membranes that have an IEC of 1.5 in the hydroxide form were synthesized for fuel cell testing at NRC. The membranes were measured and found to be relatively uniform, at 40 and 55 µm thick, respectively. Small samples of these membranes in the hydroxide form were tested for stability for a week in a solution that was nearly identical to the fuel solution at NRC, and found to be stable. Preliminary fuel cell testing results are very promising, with very good performance results. When

compared to polymers under similar conditions, as shown below in Table 9, it outperformed most similar polymers in maximum current density and had a comparable maximum power density, despite having the lowest maximum OCV. This shows that it is a promising candidate for use in AEMFCs.

Table 9: Fuel cell test comparisons of the blend membrane to other polymers.

Polymer	Anode Catalyst	Cathode Catalyst	Fuel Solution	Temperature (°C)	Maximum Power Density (mW/cm^2)	Corresponding Current Density (mA/cm^2)	Max OCV (V)
Mes-PBI and Mes-P(DMBI)-OH^- Blend	Pt/C; 30% Pt 2 mg/cm^2 loading	Acta Hypermec 1 mg/cm^2 loading	2 M EtOH/2 M KOH	60	15	8	0.55
Quaternary ammonium sulphone	Cr-Ni nanoparticles 5 mg/cm^2 loading	Silver 1 mg/cm^2 loading	Not specified	60	0.5	1	0.92
Hydroxide-doped meta-PBI	45% PtRu/C	40% MnO_2/C	2 M EtOH/2 M KOH	60	30	9	0.9
	40% Pd/C	40% MnO_2/C	2 M EtOH/2 M KOH	60	16	0.9	0.6

TGA graphs have been measured for the blends in both the iodide and hydroxide forms, for all IECs. The iodide form of the blend membrane with an IEC of 1.0, shown in Figure 3.16 (black curve), lost 7% of its mass up to 154°C, and then went through 3 decomposition stages, one between 154 – 267°C (12% mass loss), one between 267 – 318°C (4% mass loss) and one between 318 – 388°C (8% mass loss) before decomposing. The hydroxide form of the blend membrane with an IEC of 1.0, also shown in Figure 3.20 (red curve), lost 7% of its mass up to 154°C, and then it gradually

lost another 8% of its mass up to 335°C. It lost another 5% between 335 – 459°C, and then gradually decomposed.

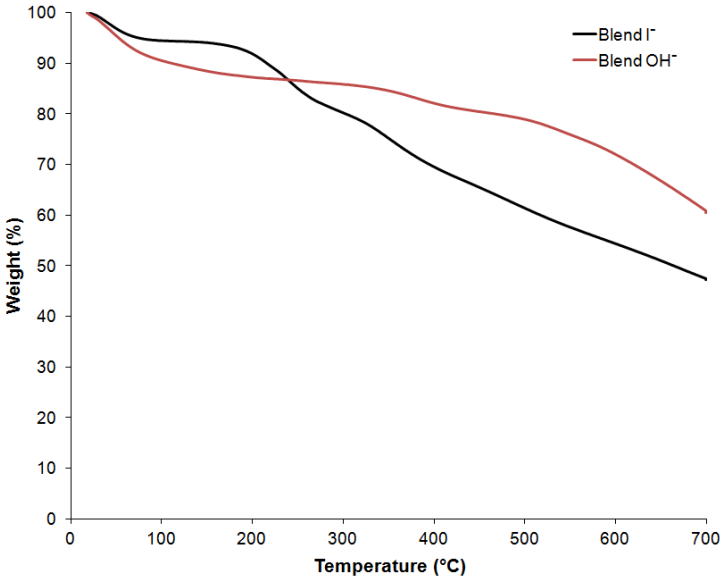

Figure 3.16: TGA plot for the blend membrane with an IEC of 1.0 in the iodide and hydroxide forms.

The iodide form of the blend membrane with an IEC of 1.5, shown in Figure 3.17 (black curve), lost 6% of its mass by 75°C, then remained at a constant mass until it went through 3 decomposition stages: one between 155 – 278°C (18% mass loss), one between 278 – 320°C (3% mass loss), and one between 320 – 400°C (8% mass loss). After that, it steadily decomposed. The hydroxide form of the blend membrane with an IEC of 1.5, also shown in Figure 3.21 (red curve), lost 11% of its mass by 78°C, and then lost another 4% of its mass between 78 – 158°C. It then gradually lost another 2% of its mass between 158 – 349°C, then another 3% of its mass between 349 – 415°C. There was one noticeable decomposition stage with a loss of 3% mass between 415 – 504°C, and after that temperature, the membrane decomposed.

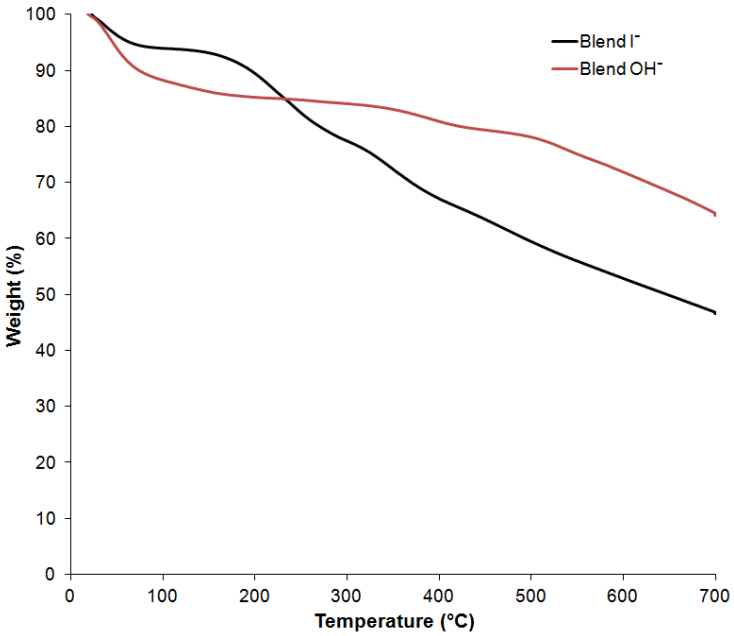

Figure 3.17: TGA plot for the blend membrane with an IEC of 1.5 in the iodide and hydroxide forms.

The iodide form of the blend membrane with an IEC of 2.0, shown in Figure 3.18 (black curve), lost 5% of its mass by 75°C and then remained steady until it underwent 2 decomposition stages, one between 157 – 331°C (20% mass loss) and one between 331 – 367°C (7% mass loss) before decomposing. The hydroxide form of the blend membrane with an IEC of 2.0, also shown in Figure 3.22 (red curve), lost 11% of its mass by 71°C, then remained steady until 337°C, where it then went through two decomposition stages, one between 337 – 418°C (4% mass loss) and one between 418 – 500°C (2% mass loss), then it decomposed.

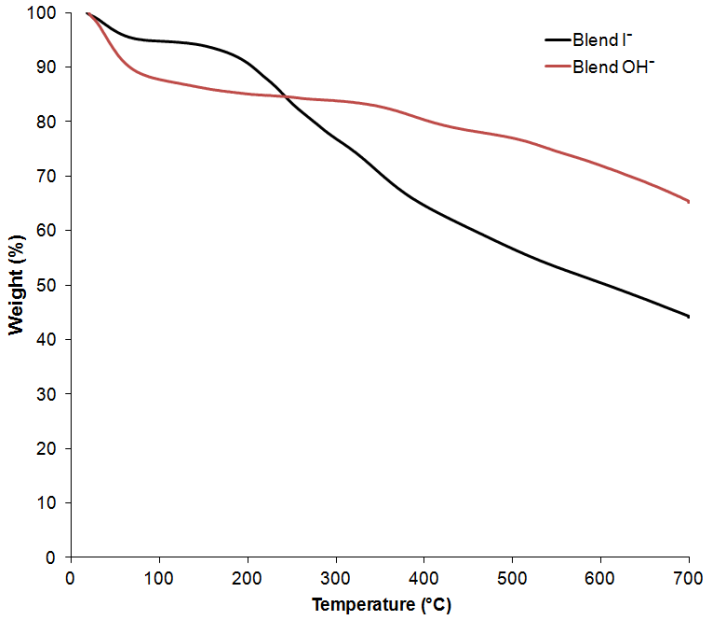

Figure 3.18: TGA plot for the blend membrane with an IEC of 2.0 in the iodide and hydroxide forms.

The iodide form of the blend membrane with an IEC of 2.5, shown in Figure 3.19 (black curve), lost 6% of its mass by 81°C, then had another 2% mass loss by 179°C. It then underwent 2 decomposition stages, one from 179 – 358°C (22% mass loss) and one between 358 – 500°C (14% mass loss) before decomposing. The hydroxide form of the blend membrane with an IEC of 2.5, also shown in Figure 3.23 (red curve), lost 9% of its mass by 71°C, then remained steady until 357°C, where it then went through two decomposition stages, one between 357 – 405°C (4% mass loss) and one between 405 – 509°C (5% mass loss), then it decomposed.

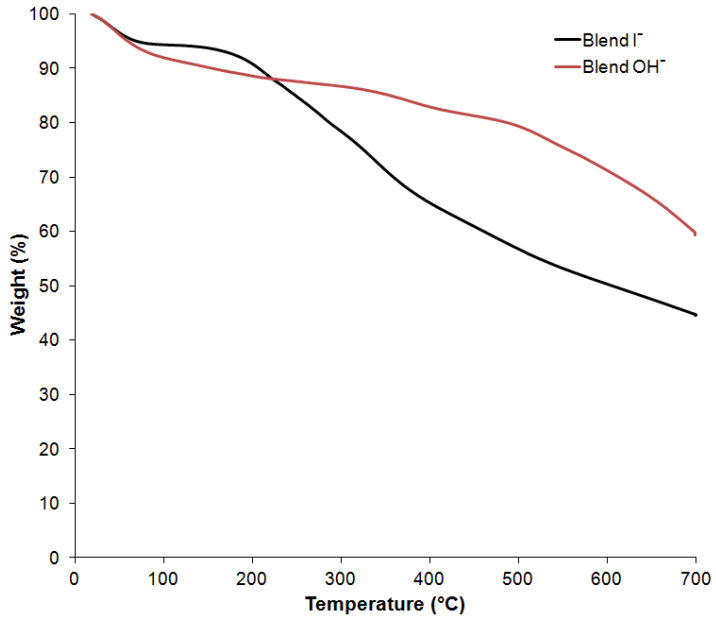

Figure 3.19: TGA plot for the blend membrane with an IEC of 2.5 in the iodide and hydroxide forms.

Overall, the blends were found to have the same decomposition pattern for the same anion, which is unsurprising given the small range of IEC values studied. The iodide blends showed marked decomposition after ~200°C, while the hydroxide membranes do not show a defined decomposition phase after ~100°C, unlike the analogous P(DMBI)-X^- membranes. This seems to suggest that the blend membranes are less stable in the hydroxide form than the iodide form.

3.5. Conclusions and Future Work

The novel polybenzimidazole Mes-P(DMBI)-X^- was successfully synthesized and found to have higher wet ionic conductivities than their corresponding P(DMBI)-X^- forms, which is likely due to the significantly higher water content. Like P(DMBI)-X^-, their properties were also anion-dependent. Of particular note is that Mes-P(DMBI)-OH^- was found to be water-soluble, but stable in elevated temperatures (60°C) and basic media (2 M $KOH_{(aq)}$).

Blend membranes of PBI and Mes-P(DMBI)-OH^- were stable and conductive in the hydroxide form, representing the first known stable benzimidazolium hydroxide-conducting polymer. The membranes had good water uptake and decent conductivity, and the membrane with an IEC of 1.5 was found to be stable for 2 weeks at 60°C in 2 M $KOH_{(aq)}$. This blend membrane also showed very promising fuel cell results.

Future work in regard to the blend membranes would involve their optimization to give the best mechanical stability and the best conductivity. Blend membranes using PBI instead of Mes-PBI could also be tried to see if the removal of the group has any effect on stability or conductivity. More rigorous fuel cell testing should also be performed on these membranes so that they can be compared to state-of-the-art existing AEMs to determine their viability in fuel cells. Lastly, the use of other alkyl groups on P(DMBI)-X^- could also be employed to stabilize the C2 carbon, preventing hydroxide attack and allowing for hydroxide conductivity.

3.6. Experimental

3.6.1. Synthesis

3.6.1.1. Materials

All materials were obtained from Sigma-Aldrich and used as-is unless otherwise stated. Bis(chloromethyl)mesitylene was purchased from Alfa Aesar Canada.

3.6.1.2. Synthesis of 2,4,6-trimethylisophthalic acid monomer

The synthesis of the 2,4,6-trimethylisophthalic acid monomer was performed according to modified literature procedures, shown in Figure 3.20.[77,79-80]

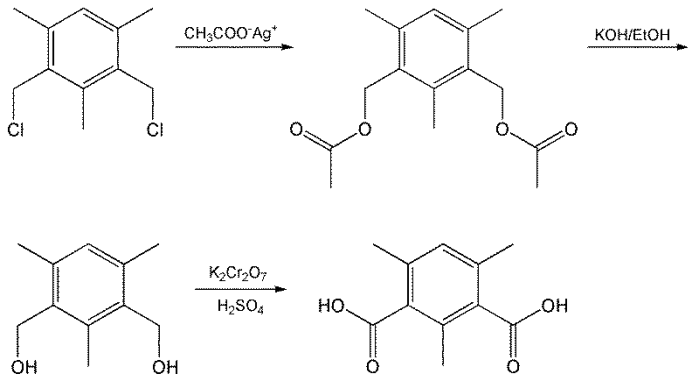

Figure 3.20: Scheme for the synthesis of 2,4,6-trimethylisophthalic acid.

10.0 g (46 mmol) of bis-(chloromethyl)-mesitylene was dissolved in 200 mL acetic acid and added to a suspension of 20.0 g silver acetate in 200 mL acetic acid in a 1 L round bottom flask. This solution was refluxed while stirring over 2 hours, then the solid was filtered away and the filtrate added to a beaker of ice. A white precipitate formed which was collected and dried (11.6 g, 95% yield). This was confirmed by IR and NMR to be bis-(acetomethyl)-mesitylene.

10.0 g (38 mmol) of bis-(acetomethyl)-mesitylene was then dissolved in 400 mL of a solution of 15% KOH in ethanol. This solution was refluxed while stirring over 2 hours, then the ethanol was removed under vacuum to yield a pale yellow solid. This solid was washed with water to remove KOH and a pale yellow powder was left behind. This was recrystallized from hot 1,4-dioxane and 5.1 g (75% yield) of needle-like white crystals were obtained. IR and NMR confirmed that it was bis-(hydroxymethyl)-mesitylene.[79]

5.0 g (28 mmol) bis-(hydroxymethyl)-mesitylene was suspended in 250 mL of acetone and stirred while Jones reagent (30 g $K_2Cr_2O_7$, 70 mL H_2O and 25 mL concentrated $H_2SO_{4(aq)}$) was slowly added at 4°C. The solution was then allowed to warm to room temperature and remained there for one hour before being heated to 40°C for 2 hours. The acetone was removed under vacuum, and a green slurry remained. This was filtered and thoroughly washed with 10% $H_2SO_{4(aq)}$, and a pale yellow sold remained. This solid was dissolved in 2 M $KOH_{(aq)}$, then activated carbon powder was added and the mixture was boiled for 30 minutes. This was filtered to remove carbon

and the filtrate was then neutralized with HCl. At low pH (< 1), a colourless solid precipitated and was filtered. This was recrystallized in acetonitrile and 4.9 g (85% yield) of short colourless crystals were recovered.

3.6.1.3. Synthesis of Mes-PBI

1.54 g (7.18 mmol) of purified 3,3'-diaminobenzidine and 60 g of polyphosphoric acid were added to a 200 mL three-necked round bottom flask fitted with an overhead stirrer, an argon inlet and a $CaCl_2$ drying tube. The flask was heated to 150°C and the solution stirred until the solid dissolved. 1.4965 g (7.18 mmol) of 2,4,6-trimethylisophthalic acid was then added and the temperature increased to 180°C for 4 hours. The temperature was then increased to 220°C for 48 hours and the solution was then poured into water to precipitate the polymer. The red solid that formed was washed thoroughly with water and a solution of $K_2CO_{3(aq)}$ to remove residual acid, and then ground into a powder which weighed 2.49 g (99% yield).[80]

3.6.1.4. Mes-P(DMBI)-I^- Synthesis

A typical scheme is shown below. 1.0 g (2.85 mmol) of Mes-PBI was dissolved in 60 mL dry DMSO at 100°C in a two-necked round bottom flask fitted with a condenser under argon. The solution was cooled to 40°C and LiH (9 mmol, 50% excess to N-H groups in polymer) was then added. The solution temperature was raised to 70°C and stirred overnight. The solution was cooled to room temperature and CH_3I (0.9 mL, 2.0 g, 10 mmol) was added. The flask was heated to 70°C for 4 hours and then a second equivalent of CH_3I (0.9 mL, 2.0 g, 10 mmol) was added. The reaction was stirred for 14 hours and then precipitated into water. The red solid was washed with water, then collected and dried under vacuum at 50°C (1.7 g, 89% yield).

3.6.2. Experimental Instrumentation

3.6.2.1. Nuclear Magnetic Resonance (NMR)

^1H NMR spectra were obtained using a 400 MHz Varian Unity Spectrometer. The polymers were dissolved in DMSO-d_6 at a concentration of ~30 mg mL^{-1}.

3.6.2.2. Thermal Gravimetric Analysis

TGA data were obtained using a TGA-50 Shimadzu Thermogravimetric analyzer. Each run was performed under nitrogen gas at a heating rate of 10°C/minute with a sample size between 20-50 mg.

3.6.2.3. Molecular Modelling

Geometry optimisations were performed with Gaussian 09 (Revision A.02) software, using B3LYP and the 6-31g* basis set on all atoms.

3.6.3. Characterization Procedures

Unless otherwise stated, all characterization procedures that were done on Mes-P(DMBI)-X^- and P(DMBI)-X^- were done in the same manner as those described in Section 2.6.3.

3.6.3.1. Anion Conductivity Measurements

The new conductivity apparatus was acquired from the Automotive Fuel Cell Corporation in Vancouver, BC, and is shown below in Figure 3.21. It is similar to the apparatus described in Figure 2.11, except that instead of using small squares of platinum for the electrode, four platinum wire electrodes run across the length of the bottom block, across which the membrane is laid. Since there are four electrodes, membranes can be cut to a smaller or larger size for measurement. The top block is screwed onto the bottom one, sandwiching the membrane in between. Each block has small holes so that the membrane can keep hydrated. The wires are attached to the apparatus using alligator clips, which clip onto the gold screws at the top that correspond to the electrodes being used.

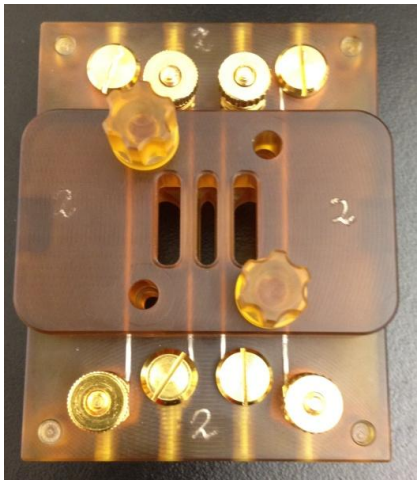

Figure 3.21: The new conductivity apparatus used for some measurements in Section 3.4.3.

References

(1) Varcoe, J. R.; Beillard, M.; Halepoto, D. M.; Kizewski, J. P.; Poynton, S. D.; Slade, R. C. T. In *Proton Exchange Membrane Fuel Cells 8*; Fuller, T., Shinohara, K., Ramani, V., Shirvanian, P., Uchida, H., Cleghorn, S., Inaba, M., Mitsushima, S., Strasser, P., Nakagawa, H., Gasteiger, H. A., Zawodzinski, T., Lamy, C., Eds.; The Electrochemical Society, 2008; Vol. 16; pp 1819-1834.

(2) Qiu, J.; Li, M.; Ni, J.; Zhai, M.; Peng, J.; Xu, L.; Zhou, H.; Li, J.; Wei, G. *Journal of Membrane Science* **2007**, *297*, 174-180.

(3) Nwal Amang, D.; Alexandrova, S.; Schaetzel, P. *Desalination* **2003**, *159*, 267-271.

(4) Du, R.; Zhao, J. *Journal of Applied Polymer Science* **2003**, *91*, 2721-2728.

(5) Wu, C.; Zhang, S.; Liu, C.; Yang, D.; Jian, X. *Journal of Membrane Science* **2008**, *311*, 360-370.

(6) Kim, I. C.; Tak, T. M. *Macromolecules* **2000**, *33*, 2391-2396.

(7) Xu, T.; Yang, W. *Journal of Membrane Science* **2001**, *183*, 193-200.

(8) Singh, S.; Jasti, A.; Kumar, M.; Shahi, V. K. *Polymer Chemistry* **2010**, *1*, 1302-1312.

(9) Strathmann, H. *Desalination* **2010**, *264*, 268-288.

(10) Mohammadi, T.; Skyllas Kazacos, M. *Journal of Power Sources* **1996**, *63*, 179-186.

(11) O'Regan, B.; Grätzel, M. *Nature* **1991**, *353*, 737-740.

(12) Nazeeruddin, M. K.; Baranoff, E.; Grätzel, M. *Solar Energy* **2011**, *85*, 1172-1178.

(13) Buraidah, M. H.; Teo, L. P.; Majid, S. R.; Arof, A. K. *Optical Materials* **2010**, *32*, 723-728.

(14) Ahn, S. H.; Kim, H. W.; Lee, S. H.; Chi, W. S.; Choi, J. R.; Shul, Y. G.; Kim, J. H. *Korean Journal of Chemical Engineering* **2011**, *28*, 138-142.

(15) Chen, C.-L.; Teng, H.; Lee, Y.-L. *Journal of Materials Chemistry* **2011**, *21*.

(16) Whittingham, M. S.; Savinell, R. F.; Zawodzinski, T. *Chemical Reviews* **2004**, *104*, 4243-4244.

(17) von Helmolt, R.; Eberle, U. *Journal of Power Sources* **2007**, *165*, 833-843.

(18) Carle, G.; Axhausen, K. W.; Wokaun, A. *Transport Reviews: A Transnational Transdisciplinary Journal* **2005**, *25*, 739-760.

(19) Cleghorn, S. J. C.; Ren, X.; Springer, T. E.; Wilson, M. S.; Zawodzinski, C.; Zawodzinski, T. A.; Gottesfeld, S. *International Journal of Hydrogen Energy* **1997**, *22*, 1137–1144.

(20) EG&G Technical Services, I. *Fuel Cell Handbook*; U.S. Department of Energy, Office of Fossil Energy, National Energy Technology Laboratory: Morgantown, 2004.

(21) Robertson, N. J.; Kostalik IV, H. A.; Clark, T. J.; Mutolo, P. F.; Abruna, H. D.; Coates, G. W. *Journal of the American Chemical Society* **2010**, *132*, 3400-3404.

(22) Kreuer, K. D. *Journal of Membrane Science* **2001**, *185*, 29-39.

(23) Salerno, H. L. S.; Beyer, F. L.; Elabd, Y. A. *Journal of Polymer Science, Part B: Polymer Physics* **2012**, *50*, 552-562.

(24) Neyerlin, K. C.; Singh, A.; Chu, D. *Journal of Power Sources* **2008**, *176*, 112-117.

(25) Hou, H.; Wang, S.; Jiang, Q.; Jin, W.; Jiang, L.; Sun, G. *Journal of Power Sources* **2011**, *196*, 3244-3248.

(26) Hou, H.; Sun, G.; He, R.; Wu, Z.; Sun, B. *Journal of Power Sources* **2008**, *182*, 95-99.

(27) Matsumoto, K.; Fujigaya, T.; Yanagi, H.; Nakashima, N. *Adv Funct Mater* **2011**, *21*, 1089-1094.

(28) Zagorodni, A. A.; Kotova, D. L.; Selemenev, V. F. *Reactive and Functional Polymers* **2002**, *53*, 157-171.

(29) Neagu, V.; Bunia, I.; Plesca, I. *Polymer Degradation and Stability* **2000**, *70*, 463-468.

(30) Wilkes, J. S.; Levisky, J. A.; Wilson, R. A.; Hussey, C. L. *Inorganic Chemistry* **1981**, *21*, 1263-1264.

(31) Chum, H. L.; Koch, V. R.; Miller, L. L.; Osteryoung, R. A. *Journal of the American Chemical Society* **1975**, *97*, 3264-3265.

(32) Ahmad, S. *Ionics* **2009**, *15*, 309-321.

(33) Liu, H.; Liu, Y.; Li, J. *Physical Chemistry Chemical Physics* **2010**, *12*, 1685-1697.

(34) Aharoni, S. M.; Signorelli, A. J. *Journal of Applied Polymer Science* **1979**, *23*, 2653-2660.

(35) Aharoni, S. M.; Litt, M. *Journal of Polymer Science, Part A: Polymer Chemistry* **1974**, *12*, 639-650.

(36) Kroschwitz, J. I. *Concise Encyclopedia of Polymer Science and Engineering*; John Wiley and Sons, 1990.

(37) Wainright, J.; Wang, J.-T.; Savinell, R. F.; Litt, M.; Moaddel, H.; Rogers, C. *Electrode Materials and Processes for Energy Conversion and Storage*: Pennington, NJ, 1995.

(38) Wainright, J. S.; Wang, J.-T.; Weng, D.; Savinell, R. F.; Litt, M. *Journal of the Electrochemical Society* **1995**, *142*, L121-L123.

(39) Xiao, L.; Zhang, H.; Jana, T.; Scanlon, E.; Chen, R.; Choe, E. W.; Ramanathan, L. S.; Yu, S.; Benicewicz, B. C. *Fuel Cells* **2005**, *5*, 287-295.

(40) Hu, M.; Pearce, E. M.; Kwei, T. K. *Journal of Polymer Science, Part A: Polymer Chemistry* **1993**, *31*, 553-561.

(41) Kim, S.-K.; Kim, T.-H.; Jung, J.-W.; Lee, J.-C. *Polymer* **2009**, *50*, 3495–3502.

(42) Kumbharkar, S. C.; Kharul, U. K. *European Polymer Journal* **2009**, *45*, 3363–3371.

(43) Kumbharkar, S. C.; Kharul, U. K. *Journal of Membrane Science* **2010**, *2010*, 134-142.

(44) Pu, H.; Liu, G. *Polymer International* **2005**, *54*, 175-179.

(45) Pu, H.; Liu, Q.; Liu, G. *Journal of Membrane Science* **2004**, *241*, 169-175.

(46) Iwakura, Y.; Uno, K.; Chau, N. *Die Makromolekulare Chemie* **1975**, *176*, 23-36.

(47) Bauer, M.; Bertario, A.; Boccardi, G.; Fontaine, X.; Rao, R.; Verrier, D. *Journal of Pharmaceutical and Biomedical Analysis* **1998**, *17*, 419-425.

(48) Jaffe, M.; Ishaq Haider, M.; Menczel, J.; Rafalko, J. *Polymer Engineering and Science* **1992**, *32*, 1236-1241.

(49) Belohlav, L. R. *Angewandte Makromolekulare Chemie* **1974**, *40*, 465-483.

(50) Samms, S. R.; Wasmus, S.; Savinell, R. F. *Journal of the Electrochemical Society* **1996**, *143*, 1225-1232.

(51) Henkensmeier, D.; Cho, H.-R.; Kim, H.-J.; Kirchner, C. N.; Leppin, J.; Dyck, A.; Jang, J. H.; Cho, E.; Nam, S.-W.; Lim, T.-H. *Polymer Degradation and Stability* **2012**, *97*, 264-272.

(52) Chatfield, D. A.; Einhorn, I. N. *Journal of Polymer Science, Part A: Polymer Chemistry* **1981**, *19*, 601-618.

(53) Ehlers, G. F.; Fisch, K. R.; Powell, W. R.; OH., A. F. M. L. W.-P. A. *Studies of the Breakdown Mechanism of Polymers. V. The Thermal Decomposition of Some Polybenzimidazoles*; Defense Technical Information Center, 1970.

(54) Dobbs, W.; Douce, L.; Heinrich, B. *Beilstein Journal of Organic Chemistry* **2009**, *5*.

(55) Gao, Y.; Twamley, B.; Shreeve, J. M. *Inorganic Chemistry* **2004**, *43*, 3406-3412.

(56) Lorgouilloux, Y.; Dodin, M.; Paillaud, J.-L.; Caullet, P.; Michelin, L.; Josien, L.; Ersen, O.; Bats, N. *Journal of Solid State Chemistry* **2009**, *182*, 622-629.

(57) Dobbs, W.; Douce, L.; Allouche, L.; Louati, A.; Malbosc, F.; Welter, R. *New Journal of Chemistry* **2006**, *30*, 528-532.

(58) Fouchet, J.; Douce, L.; Heinrich, B.; Welter, R.; Louati, A. *Beilstein Journal of Organic Chemistry* **2009**, *5*.

(59) Busto, E.; Gotor-Fernandez, V.; Rıos-Lombardı, N.; Garcıa-Verdugo, E.; Alfonso, I.; Garcıa-Granda, S.; Menendez-Velazquez, A.; Burguete, M. I.; Luis, S. V.; Gotor, V. *Tetrahedron Letters* **2007**, *48*, 5251-5254.

(60) Gao, Y.; Ye, C.; Twamley, B.; Shreeve, J. M. *Chemistry - A European Journal* **2006**, *12*, 9010-9018.

(61) Perkin Elmer, 2010; pp 19.

(62) Oxtoby, D. W.; Nachtrieb, N. H. *Principles of Modern Chemistry*; Saunders College Publishing: New York, 1985.

(63) Peckham, T. J.; Schmeisser, J.; Holdcroft, S. *Journal of Physical Chemistry B* **2008**, *112*, 2848-2858.

(64) Peckham, T. J.; Schmeisser, J.; Rodgers, M.; Holdcroft, S. *Journal of Materials Chemistry* **2007**, *17*, 3255-3268.

(65) Atkins, P. W. *Physical Chemistry*; 4 ed.; W.H. Freeman and Company: New York, 1990.

(66) Paddison, S. J. *Journal of New Materials for Electrochemical Systems* **2001**, *4*, 197-207.

(67) Adamson, A. A. *A Textbook of Physical Chemistry*; Academic Press, Inc.: New York, 1973.

(68) Yan, J.; Hickner, M. A. *Macromolecules* **2010**, *43*, 2349-2356.

(69) Lee, S.-H. A.; Jackson, A.-M. S.; Hess, A.; Fei, S.-T.; Pursel, S. M.; Basham, J.; Grimes, C. A.; Horn, M. W.; Allcock, H. R.; Mallouk, T. E. *Journal of Physical Chemistry C* **2010**, *114*.

(70) Han, H.; Liu, W.; Zhang, J.; Zhao, X.-Z. *Adv Funct Mater* **2005**, *15*, 1940-1944.

(71) Souquet, J.-L.; Duclot, M.; Levy, M. *Solid State Ionics* **1996**, *85*, 149-157.

(72) Duclot, M.; Alloin, F.; Brylev, O.; Sanchez, J. Y.; Souquet, J. L. *Electrochimica Acta* **2005**, *50*, 5015-5021.

(73) Ma, Y.-L.; Wainright, J. S.; Litt, M. H.; Savinell, R. F. *Journal of the Electrochemical Society* **2004**, *151*, A8-A16.

(74) Druin, M. L.; Oringer, K.; Celanese Corporation: United States of America, 1976; pp 6.

(75) Kerres, J.; Ullrich, A.; Meier, F.; Haring, T. *Solid State Ionics* **1999**, *125* 243–249.

(76) Thomas, O. D.; Peckham, T. J.; Thanganathan, U.; Yang, Y.; Holdcroft, S. *Journal of Polymer Science, Part A: Polymer Chemistry* **2010**, *48*, 3640-3650.

(77) Thomas, O. D., Simon Fraser University, 2011.

(78) Thomas, O. D.; Soo, K. J. W. Y.; Peckham, T. J.; Kulkarni, M.; Holdcroft, S. *Journal of the American Chemical Society* **2012**, *134*, 10753-10756.

(79) Rhoad, M. J.; Flory, P. J. *Journal of the American Chemical Society* **1950**, *72*, 2216-2219.

(80) Kolotuchin, S. V.; Thiessen, P. A.; Fenlon, E. E.; Wilson, S. R.; Loweth, C. J.; Zimmerman, S. C. *Chemistry - A European Journal* **1999**, *5*, 2537-2547.

(81) Freiser, B. S.; Woodin, R. L.; Beauchamp, J. L. *Journal of the American Chemical Society* **1975**, *97*, 6893-6894.

(82) Zoltewicz, J. A.; Helmick, L. S. *Journal of the American Chemical Society* **1970**, *92*, 7547-7552.

(83) Jung, M.-s. J.; Arges, C. G.; Ramani, V. *Journal of Materials Chemistry* **2011**, *21*, 6158-6160.

(84) Ye, Y.; Elabd, Y. A. *Macromolecules* **2011**, *44*, 8494–8503.

(85) Lin, B.; Qiu, L.; Lu, J.; Yan, F. *Chemistry of Materials* **2010**, *22*, 6718-6725.

(86) Hibbs, M. R.; Fujimoto, C. H.; Cornelius, C. J. *Macromolecules* **2009**, *42*, 8316-8321.

(87) Peckham, T. J.; Holdcroft, S. *Advanced Materials* **2010**, *22*, 4667-4690.

Appendix

Calculation of Masses of Starting Material Needed

For all blend membranes, the target mass was 0.200 g in the hydroxide form.

$$\text{IEC} = \left(\frac{\text{moles of anion}}{\text{mass of one polymer repeat unit}}\right) \text{x } 1000$$

The IECs of the polymers are as follows:

$$\text{Mes} - \text{PBI} = \left(\frac{2 \text{ moles}}{350.184 \text{ g}}\right) \text{x } 1000 = 5.71 \text{ meq/g}$$

$$\text{Mes} - \text{P(DMBI)} - \text{I}^- = \left(\frac{2 \text{ moles}}{664.049 \text{ g}}\right) \text{x } 1000 = 3.01 \text{ meq/g}$$

$$\text{Mes} - \text{P(DMBI)} - \text{OH}^- = \left(\frac{2 \text{ moles}}{442.28 \text{g}}\right) \text{x } 1000 = 4.52 \text{ meq/g}$$

To obtain a blend membrane with a final IEC of 2.5 in the hydroxide form, the following calculations were performed:

Blend membrane final IEC = x(IEC of Mes-P(DMBI)-OH^-) + (1 – x)(-IEC of Mes-PBI)

where x is equal to the percentage of Mes-P(DMBI)-OH^- by mass in the blend membrane.

2.5 = x(4.52) + (1-x)(-5.71)

2.5 = 4.52x – 5.71 + 5.71x

2.5 + 5.71 = 4.52x + 5.71x

8.21 = 10.23x

x = 0.8025

For a membrane with a final mass of 0.200 g in the hydroxide form:

Mass of Mes-P(DMBI)-OH^- = 0.8025(0.200 g) = 0.1605 g

To calculate the corresponding mass of Mes-P(DMBI)-I^-, the moles of anion do not change when converting from I- to OH-, therefore:

1 mol (Mes-P(DMBI)-OH^-) = 1 mol (Mes-P(DMBI)-I^-)

1 g (Mes-P(DMBI)-OH^-) = $\frac{1\ g}{442.28\ g/mol}$ = 0.00226 mol

This is equivalent to the moles of (Mes-P(DMBI)-I^-), so the equivalent mass is:

0.00226 mol (664.049 g/mol) = 1.50 g.

So if 0.40125 g Mes-P(DMBI)-OH^- are needed, then (0.1605 g)(1.50) = 0.24075 g of Mes-P(DMBI)-I^- are needed.

The mass of Mes-PBI needed for this blend:

Mass (Mes-PBI) = (0.200 g)(1-0.8025) = 0.0395 g.

Calculation of Blend IEC in the iodide form

For a blend with an IEC of 2.5 in the hydroxide form, it contains 0.0395 g Mes-PBI and 0.2408 g Mes-P(DMBI)-I^-), for a total mass of 0.2803 g in the iodide form. The IEC of Mes-P(DMBI)-I^-) is 3.01, which is the only contributor to the IEC in the iodide form as no cross-links are formed. So the IEC in the iodide form is:

$$\text{IEC} = \frac{3.01 \text{ meq/g x } 0.2408 \text{ g}}{0.2803 \text{ g}} = 2.59\ meq/g$$